TABLE 1. Cool Star Absorption Strengths

Name	SpType[a]	"Na"[b] (Å)	"Ca"[c] (Å)	CO[d] (%)	H_2O[e] (%)
SU Per[f]	M3–4 Iab	6.8 ± 0.2	4.2 ± 0.2	27.1 ± 0.1	6.1 ± 0.2
KY Cyg[g]	M3 Ia	6.7 ± 0.3	4.1 ± 0.3	25.3 ± 0.2	9.6 ± 0.2
SAO119[g]	M3 Ia	7.1 ± 0.3	4.8 ± 0.3	21.4 ± 0.2	-2.5 ± 0.2
PZ Cas[g]	M4 Ia	6.5 ± 0.4	4.2 ± 0.3	23.7 ± 0.2	5.1 ± 0.3
RT Car	M2+ Ia	4.4 ± 0.8	3.5 ± 0.7	24.8 ± 0.5	5.3 ± 0.5
α Ori[h,i]	M2 Iab	6.5 ± 0.0	4.7 ± 0.0	24.6 ± 1.2	-0.2 ± 1.3
μ Cep[f]	M2 Ia	6.2 ± 0.2	3.9 ± 0.2	24.6 ± 0.1	5.2 ± 0.2
HR 8726[f]	K5 Ib	4.8 ± 0.2	3.3 ± 0.2	17.4 ± 0.1	2.6 ± 0.2
R Leo[h]	M8e, Mira	$\cdots$	$\cdots$	20.2 ± 0.5	16.3 ± 0.5
R Cas[h]	M7e, Mira	$\cdots$	$\cdots$	21.1 ± 0.8	20.4 ± 0.8
R Hyd[h]	M7e, Mira	$\cdots$	$\cdots$	17.6 ± 0.8	6.7 ± 0.8
o Cet[h,i]	M6e, Mira	5.8 ± 0.0	5.3 ± 0.0	20.5 ± 0.8	15.2 ± 0.8
χ Cyg[h,i]	S6$^+$/1e, Mira	7.7 ± 0.0	4.6 ± 0.0	20.5 ± 0.8	$\cdots$
BK Vir[f]	M7− III	6.7 ± 0.2	4.1 ± 0.2	19.8 ± 0.1	10.3 ± 0.1
SW Vir[f]	M7 III	6.2 ± 0.2	4.7 ± 0.2	17.6 ± 0.1	11.1 ± 0.1
HD 207764	M7 III	6.6 ± 0.5	4.1 ± 0.4	17.8 ± 0.3	4.3 ± 0.3
R Lyra[f]	M5 III	6.4 ± 0.2	4.4 ± 0.2	17.7 ± 0.1	3.6 ± 0.2
HD 212275	M3 III	4.7 ± 0.4	3.5 ± 0.3	16.3 ± 0.2	2.1 ± 0.3
χ Peg[f]	M2 III	4.7 ± 0.2	3.1 ± 0.2	14.2 ± 0.1	2.3 ± 0.2
γ Sge[f]	M0 III	4.1 ± 0.2	3.0 ± 0.2	12.6 ± 0.1	1.8 ± 0.2
HD 212895	M0 III	4.1 ± 0.4	2.6 ± 0.3	12.8 ± 0.2	-2.1 ± 0.3
HD 89060[j]	M4 III	6.2 ± 0.3	4.3 ± 0.3	15.9 ± 0.2	7.2 ± 0.2
HD 89951[j]	M3 III	4.9 ± 0.2	3.9 ± 0.2	15.0 ± 0.1	5.7 ± 0.2
HD 94152[j]	M6 III	5.2 ± 0.2	3.1 ± 0.2	16.9 ± 0.1	12.5 ± 0.1
HD 99495[j]	M4 III	5.7 ± 0.3	4.3 ± 0.3	15.6 ± 0.2	8.2 ± 0.2
HD 100569[j]	M2 III	3.7 ± 0.2	3.7 ± 0.2	13.3 ± 0.1	5.8 ± 0.2
HD 100783[j]	M2 III	4.1 ± 0.2	3.5 ± 0.2	13.1 ± 0.1	5.4 ± 0.2
HD 102608[j]	M7 III	6.3 ± 0.2	4.6 ± 0.2	16.7 ± 0.1	12.4 ± 0.1
HD 102766[j]	M6 III	6.4 ± 0.2	4.5 ± 0.2	19.1 ± 0.1	11.8 ± 0.1
HD 104745[j]	M3 III	5.0 ± 0.2	3.6 ± 0.2	16.7 ± 0.1	11.8 ± 0.1
HD 109225[j]	M5 III	5.1 ± 0.3	3.3 ± 0.3	14.1 ± 0.2	8.1 ± 0.2
HD 109467[j]	M6 III	5.2 ± 0.3	3.7 ± 0.3	15.3 ± 0.2	8.4 ± 0.2
RT Vir[j]	M8 III	6.9 ± 0.3	5.3 ± 0.3	16.6 ± 0.2	16.6 ± 0.2
HD 126903[j]	M6 III	5.1 ± 0.5	5.2 ± 0.5	16.9 ± 0.3	9.2 ± 0.3
BW 4-028[j]	M7 III	6.2 ± 0.3	3.8 ± 0.3	16.6 ± 0.2	15.1 ± 0.2
BW 4-055[j]	M8 III	8.0 ± 0.4	5.3 ± 0.3	18.7 ± 0.2	18.5 ± 0.2
BW 4-78[j]	M5 III	4.6 ± 0.2	4.7 ± 0.2	15.2 ± 0.1	6.4 ± 0.2
BW 4-93[j]	M6 III	6.5 ± 0.5	4.4 ± 0.5	17.5 ± 0.3	6.8 ± 0.4
BW 4-107[j]	M6 III	9.0 ± 0.1	6.6 ± 0.1	14.3 ± 0.0	1.7 ± 0.1
BW 4-133[j]	M6 III	6.2 ± 0.5	$\cdots$	17.2 ± 0.3	6.6 ± 0.4
BW 4-165[j]	M7 III	7.6 ± 0.6	5.8 ± 0.5	19.0 ± 0.4	8.4 ± 0.4
BW 4-179[j]	M7 III	8.0 ± 0.2	5.1 ± 0.2	18.1 ± 0.1	10.8 ± 0.1
BW 4-247[j]	M8 III	7.6 ± 0.3	5.4 ± 0.3	17.5 ± 0.2	13.3 ± 0.2
BW 4-289[j]	M9 III	7.9 ± 0.5	5.8 ± 0.4	19.9 ± 0.3	13.0 ± 0.3
IRS 1NE	K5–M0 I or M7 III	7.3 ± 1.2	5.4 ± 1.0	18.4 ± 0.7	$\cdots$
IRS 1SE	K5 I or M7 III	8.2 ± 1.3	5.0 ± 1.1	17.3 ± 0.8	1.4 ± 0.9
IRS 2	K5 I or M7 III	$\cdots$	$\cdots$	16.7 ± 0.9	$\cdots$
IRS 7[k]	M1 I	8.6 ± 0.4	5.8 ± 0.3	22.1 ± 0.2	2.0 ± 0.3

TABLE 1. (continued)

Name	SpType[a]	"Na"[b] (Å)	"Ca"[c] (Å)	CO[d] (%)	H$_2$O[e] (%)
IRS 9	> M7 III	6.7 ± 1.4	5.5 ± 1.2	23.0 ± 0.8	16.1 ± 0.9
IRS 11	> M7 III	7.9 ± 0.5	5.6 ± 0.4	21.3 ± 0.3	9.1 ± 0.3
IRS 12N	> M7 III	8.4 ± 1.6	5.7 ± 1.3	23.0 ± 0.9	14.3 ± 1.5
IRS 12S	M6 III	6.0 ± 1.2	3.7 ± 1.0	17.1 ± 0.7	13.5 ± 0.7
IRS 14NE	M7 III	8.8 ± 2.4	⋯	19.1 ± 1.5	13.3 ± 1.5
IRS 19[k]	M0 I	6.2 ± 0.6	6.1 ± 0.5	20.7 ± 0.4	5.7 ± 0.4
IRS 20	M7 III	6.5 ± 1.2	5.9 ± 1.1	19.3 ± 0.8	4.6 ± 0.8
IRS 22[k]	M1 I	7.6 ± 0.8	6.4 ± 0.7	21.3 ± 0.5	5.4 ± 0.5
IRS 23[k]	> M7 III	6.2 ± 0.4	3.2 ± 0.3	14.3 ± 0.2	16.1 ± 0.2
IRS 24[l]	> M7 III	6.0 ± 0.6	3.9 ± 0.5	22.6 ± 0.4	12.9 ± 0.4
IRS 28	> M7 III	8.8 ± 0.7	8.2 ± 0.6	22.6 ± 0.4	16.3 ± 0.4
OSU C1	M7 III	9.3 ± 1.6	5.7 ± 1.3	19.0 ± 0.9	⋯
OSU C2	M7 III	8.8 ± 1.3	8.1 ± 1.1	19.4 ± 0.8	11.6 ± 0.9
OSU C3	M0–1 I or > M7 III	7.1 ± 1.2	6.1 ± 1.1	22.0 ± 0.7	⋯
OSU C4	> M7 III	9.4 ± 2.6	⋯	22.0 ± 1.5	⋯

[a]Spectral type taken from same reference as spectrum for disk and bulge stars. RT Car spectral type from Humphreys (1978). OSIRIS M III spectral types are from the Michigan Spectral Catalog. For the Galactic center stars, spectral type is estimated based on the analysis of the Galactic center spectra and M_K. M III refers to both AGB and LPV stars; see text, Table 2.

[b]Equivalent width (W_λ) in 0.015 μm wide band centered at 2.206 μm, near the Na I doublet. "Na" refers to the fact that this feature is near the Na doublet, but more than half of the W_λ may be due to Sc, Ti, Si, and V; see text.

[c]W_λ in 0.013 μm wide band centered at 2.264 μm, near the Ca I triplet. "Ca" refers to the fact that this feature is near the Ca triplet, but more than half of the W_λ may be due to Fe, Ti, and Sc; see text.

[d]CO 2–0 rotational vibrational band. Absorption strength is defined as $(1 - F_{CO}/F_{cont}) \times 100$, where F_{CO} and F_{cont} are the integrated flux in 0.015 μm bands centered at 2.302 μm and 2.284 μm, respectively.

[e]H$_2$O absorption strength defined as $(1 - F_{H_2O}/F_{cont}) \times 100$, where F_{H_2O} and F_{cont} are the integrated flux in 0.015 μm bands located at 2.095 μm and 2.284 μm, respectively. Only Galactic center stars with A_K determined from two or more infrared colors (Paper I) have measured H$_2$O.

[f]Spectrum taken from Kleinmann & Hall (1986) and re–binned to 19.4 Å pix^{-1}; see text.

[g]Spectrum taken from Hanson et al. (1996). Spectra are $\sim$ 16 Å pix^{-1}, not re–binned.

[h]Spectrum taken from Johnson & Méndez (1970). Spectra are $\sim$ 40 Å pix^{-1}, not re–binned.

[i]"Na" and "Ca" measured from high resolution spectra of Wallace & Hinkle (1996).

[j]Spectrum taken from Terndrup et al. (1991). Spectra are 22 Å pix^{-1}, not re–binned. BW stars have grism spectral types which may be different than MK types; see Terndrup et al. (1990).

[k]Spectra taken from Sellgren et al. (1987) and re–binned to 19.4 Å pix^{-1}; see text. Absorption strengths for IRS 19 and 22 are unweighted averages of values derived from the OSIRIS spectra and re–binned Sellgren et al. spectra.

[l]Spectrum taken from Levine et al. (1995). Spectrum is 16 Å pix^{-1}, not re–binned.

Notes to Table 1.

Spectra are from this paper unless otherwise noted.

Really Cool Stars at the Galactic Center

R. D. Blum[1,2]

JILA, University of Colorado

Campus Box 440, Boulder, CO, 80309

rblum@casa.colorado.edu

K. Sellgren[1,3] and D. L. DePoy[1]

Department of Astronomy, The Ohio State University

174 W. 18th Ave., Columbus, Oh, 43210

sellgren@payne.mps.ohio-state.edu

depoy@payne.mps.ohio-state.edu

ABSTRACT

New and existing $K-$band spectra for 19 Galactic center late–type stars have been analyzed along with representative spectra of disk and bulge M giants and supergiants. Absorption strengths for strong atomic and molecular features have been measured. The Galactic center stars generally exhibit stronger absorption features centered near Na I (2.206 μm) and Ca I (2.264 μm) than representative disk M stars at the same CO absorption strength.

Based on the absolute $K-$band magnitudes and CO and H_2O absorption strengths for the Galactic center stars and known M supergiants and asymptotic giant branch (AGB) stars, we conclude that only IRS 7 must be a supergiant. Two other bright stars in our Galactic center sample are likely supergiants as well. The remaining bright, cool stars in the Galactic center that we have observed are most consistent with being intermediate mass/age AGB stars. We identify five of the Galactic center stars as long period variables based on their $K-$band spectral properties and associated photometric variability. Estimates of initial masses and ages for the GC stars suggest multiple epochs of star formation have occurred in the Galactic center over the last 7–100 Myr.

---

1. INTRODUCTION

Blum et al. (1996, hereafter Paper I) presented near infrared photometry for the Galactic center (GC) stellar population (within the central $\sim$ 4–5 pc). Analysis of the $JHKL$ photometry showed an excess component of bright stars in the stellar population compared to the population in the nearby bulge field known as Baade's window (BW, $l, b =$ $1°, -4°$).

This excess of bright stars has been known for some time (see the discussion in Paper I and references therein) and is generally attributed to recent star formation resulting in younger, more massive stars than exist in BW. Substantial evidence for very recent star formation ($\lesssim$8 Myr) has come from studies of hot emission–line stars in the GC (Forrest et al. 1987; Allen et al. 1990; Krabbe et al. 1991; Libonate et al. 1995; Blum et al. 1995a, b; Krabbe et al. 1995; Figer 1995; Tamblyn et al. 1996). These stars are thought to be post-main-sequence objects with initial masses > 35 $M_\odot$. But, as pointed out in Paper I, based on published spectra and the spectra we present here, the emission–line stars are not the most conspicuous stars in the GC bright component. The brightest GC stars at K are largely stars identified as being cool M stars.

An important distinction between the cool and hot stars is that the luminous cool stars can trace the most recent epochs of star formation (red supergiants) as well as older ones (M giants and intermediate age asymptotic giant branch stars), while the hot stars trace only the former. In this paper, we extend the work begun by Lebofsky et al. (1982, hereafter LRT) and Sellgren et al. (1987, hereafter S87) which sought to identify the most luminous M stars in the GC as massive red supergiants or less massive giants and so trace star formation there. Our new spectroscopy (this paper) and photometry (Paper I) are of higher angular resolution than these earlier studies. The spectra presented here sample GC stars in the brightest five magnitudes of the observed $K-$band luminosity function (Paper I). We will also discuss the GC cool stars in the context of asymptotic giant branch (AGB) stars, the most luminous of which are long period variables (LPVs). This is particularly relevant in light of the fact that photometric variables have recently been identified in the GC (Haller 1992; Tamura et al. 1994, 1996; Paper I).

2. OBSERVATIONS AND DATA REDUCTION

The GC observations were obtained on the nights of 1993 July 11−13 on the 4–m telescope at the Cerro Tololo Inter–American Observatory (CTIO) using the Ohio State Infrared Imager and Spectrometer (OSIRIS). Spectra of three disk M giants were obtained

with OSIRIS on the CTIO 4–m during the night of 1994 June 28. OSIRIS is described by DePoy et al. (1993). All basic data reduction procedures were accomplished using IRAF.[4]

Observations and data reduction of the OSIRIS GC $K-$band spectra taken in 1993 July have been discussed in detail by Blum et al. (1995b). Briefly, these R $(= \lambda/\Delta\lambda) \sim$ 570 (19.4 Å pix^{-1}) spectra were extracted from 0.4$''$ pix^{-1} long slit images (slit oriented E–W) of the central $102'' \times 10''$ of the Galaxy (slit width ~ 1.2"). We also obtained long slit images centered on several additional stars up to $\sim 30''$ from the center. The GC spectra were obtained in seeing of $\sim 1'' - 1.5''$. Each frame was flat–fielded and sky subtracted; this included a secondary flat–field to account for scattered light (see Blum et al. 1995b). The sky images were taken at positions $500'' - 600''$ off the GC. In addition, local background apertures were also used to subtract diffuse emission and the underlying stellar background. Each extracted spectrum was also divided by the spectrum of an A or B star to correct for telluric absorption. Prior to this correction, the Brγ (2.16 μm) absorption in the A and B stars was removed by estimating a continuum across it by eye.

Spectra for one supergiant (1993 July) and three disk M giants (1994 June) listed in Table 1 were obtained with the same instrumental setup as the GC OSIRIS spectra. The supergiant RT Car was observed with a neutral density filter. The reduction was similar to the GC stars with the exception that no secondary flat–field was used for the 1994 June data since additional baffling in OSIRIS and improved observing procedures (see the discussion on the high resolution spectrum of IRS 13 in Blum et al. 1995b) eliminated the effects of scattered light.

Table 1 also includes spectra of three disk supergiant stars, five disk M giants, and GC stars from Kleinmann & Hall (1986; hereafter KH) and S87 which have been re–binned to the same resolution as the OSIRIS data. These high resolution spectra were first re–binned to the 19.4 Å pix^{-1} sampling of the OSIRIS spectra, then each data point was replaced with the weighted average of its two neighbors and itself (weights: 0.5, 0.5, 1.0). A spectrum of the GC star IRS 24 (19 Å pix^{-1}, not re–binned) was kindly provided by D. Levine and D. Figer and included in our sample. This spectrum was previously published by Levine et. al (1995). The GC star and disk star spectra taken with OSIRIS and the IRS 7, IRS 23, IRS 24, and μ Cep spectra are shown in Figure 1. All spectra in this figure have been de–reddened according to the A_K values given in Table 4 of Paper I and are presented as the normalized ratio of the stellar spectrum to the hot star spectrum used in correcting telluric absorption.

We also make use of spectra of 14 field M giants and 10 BW M giants from Terndrup

---

[4] IRAF is distributed by the National Optical Astronomy Observatories.

et al. (1991), three supergiants from Hanson et al. (1996), and FTS spectra of five Mira stars (LPVs) and one M supergiant from Johnson & Méndez (1970). All these stars are listed in Table 1. These spectra (22 Å pix^{-1}, 16 Å pix^{-1}, and $\sim$ 40 Å pix^{-1}, respectively) were not re–binned. The bulge and LPV stars were normalized in the same way as the GC and disk stars before analysis. A plot of the Johnson & Méndez spectrum of R Cas (M7e, Mira) is shown in Figure 1.

The disk giants and supergiants were used to compare measured atomic absorption feature strengths to similar measures in the GC stars. Equivalent widths (W$_\lambda$) were measured in bands centered near the Na I doublet ($\lambda \approx 2.206$ μm, $\Delta\lambda = 0.015$ μm) and the Ca I triplet ($\lambda \approx 2.264$ μm, $\Delta\lambda = 0.013$ μm). A linear continuum was calculated across each feature by interpolating between nearby continuum positions on either side of each feature. Inspection of the high resolution and re–binned KH and S87 spectra shows that the W$_\lambda$ for both the Na I and Ca I features have contributions from other absorption features. Hereafter, we will refer to the atomic measurements as "Na" and "Ca" due to the contributions of multiple species to the absorption strength (see § 3.3 for details of the additional contributors). Due to the more coarse sampling of the Johnson & Méndez (1970) stars and their generally lower signal–to–noise, we did not attempt to make "Na" and "Ca" measurements for them. Instead, we supplemented two of these stars with measurements of "Na" and "Ca" from the high resolution atlas of Wallace & Hinkle (1996). The spectra for these two stars (o Cet and α Ori) were re-binned to the OSIRIS resolution.

In addition to the atomic line measures, we computed absorption strength measurements for the CO bandhead at 2.2935 μm and for H$_2$O near the blue end of the spectra. Both of these measures were computed as the percentage of flux in the band relative to a continuum band at 2.284 μm ($[1 - F_{band}/F_{cont}] \times 100$). All three fluxes were measured in 0.015 μm wide bands. The CO band was placed with its center at 2.302 μm and the H$_2$O band was centered at 2.095 μm. Our CO and H$_2$O indices are not the same as the more well known narrow–band photometric indices (e.g., Frogel et al. 1978), but they are correlated with the photometric indices. See the discussion below on the correlation between the our indices and those of KH which have, inturn, been shown by KH to be correlated with the narrow–band indices.

The uncertainties reported in Table 1 were derived by taking the rms deviation in regions between features as the uncertainty in a single pixel and then propagating this uncertainty through the definitions of the absorption measures. The absorption strengths were calculated after de–reddening the spectra. Each GC spectrum was de-reddened using the estimates of A_K in Table 4 of Paper I and the interstellar extinction curve of Mathis (1990). The BW stars were de-reddened by $A_K = 0.14$ mag (Frogel & Whitford 1987,

hereafter FW87); none of the disk giants or LPVs include correction for extinction. The reddening of the supergiants was estimated either from their observed colors (Hoffleit 1982; Nicolet 1978) and assumed intrinsic colors (Johnson 1966), or was adopted from Elias et al. (1986, hereafter EFH). We corrected the supergiants for extinction values of $A_K = 0.1 - 0.6$ using a Mathis (1990) extinction curve with $R = 3.1$.

The atomic absorption feature equivalent widths are unaffected by extinction. The CO strengths are affected only marginally since the bands are close together. The formal uncertainty in the CO strength due to uncertainty in A_K can be expressed as $\Delta CO/\Delta A_K$ = $1.0 \times (1 - CO)$ % mag^{-1}. The CO strength is underestimated if A_K is underestimated. The H_2O strengths are more dependent on the derived reddening because of the large wavelength difference between the flux and continuum bands. In this case, $\Delta H_2O/\Delta A_K =$ $-13.8 \times (1 - H_2O)$ % mag^{-1}. The H_2O strength is overestimated if A_K is underestimated.

The re–binned disk star spectra show similar absorption strengths as the disk stars of the same spectral type which have spectra taken on the OSIRIS system (see Table 1), suggesting that one–to–one comparisons can be made for "Na," "Ca," and CO absorption strengths measured on these different systems. Comparison of similar spectral type data data for disk stars from KH and this paper to the disk stars from Terndrup et al. (1991), however, shows slightly redder continua. This means that the H_2O values for the Terndrup et al. (1991) disk stars may be a few percent larger than the other disk stars of similar spectral type in our sample. We do not consider the difference in observed H_2O strengths significant, however, due to the small number of stars in each sample. For M5 – M7 giants, the Terndrup et al. giants have a mean H_2O of 10.4 % $\pm$ 0.9 % compared to 7.3 % $\pm$ 2.3 % for the re–binned KH and OSIRIS giants.

Our measurements of the CO and H_2O strengths for the re–binned KH spectra correlate very well with the the published KH indices. We find that the CO index of KH, CO_{KH}, is related to our CO strength values derived from the re–binned KH spectra, CO_{rebin}, as follows: $CO_{KH} = a + (b \times CO_{rebin})$, with $a = 8.90 \pm 1.31$ and $b = 1.27 \pm 0.07$. Our H_2O strength measurements also agree well with those of KH, with a mean difference between our measurements of the re-binned KH spectra and the KH H_2O indices of -0.4 $\pm$ 0.4 % (comparing before extinction correction since KH made no correction). We find, however, that the "Na" and "Ca" indices of KH are systematically underestimated for stars with strong H_2O absorption, such as BK Vir and SW Vir. This is because KH adopted a continuum for the "Na" and "Ca" indices which was interpolated linearly between two widely separated regions in the blue half of the K band, and this continuum is therefore affected by the amount of H_2O absorption. Our "Na" and "Ca" equivalent widths are derived using a local continuum, and therefore are not as sensitive to the amount of H_2O

absorption (the presence of many weak H_2O lines might affect the overall level of the continuum, Wallace & Hinkle 1996). We find good agreement of our "Na" and "Ca" equivalent widths, measured from the original Terndrup et al. (1991) spectra, with the "Na" and "Ca" equivalent widths published by Terndrup et al. (1991). All absorption measurements were computed using the LINER spectral analysis program in use at Ohio State.

3. RESULTS

3.1. Comparison with Previous GC Spectra

Spectra for some of the GC cool stars in this paper have been presented previously (LRT; S87; Rieke et al. 1989; Krabbe et al. 1995). The OSIRIS spectra presented in Figure 1 are higher spatial resolution than LRT, S87, and Rieke et al. (1989), and similar to Krabbe et al. (1995). Analysis of our $K-$band images (Paper I) shows that many of the spectra presented in earlier, lower angular resolution work must have been contaminated by neighboring stars (particularly sources IRS 11, 12, 19, 22, 23, and 24). For example, there is a star $\sim 1.8''$ SW of IRS 11 and only 0.5 mag fainter (at K) which must have contaminated the S87 IRS 11 spectrum ($3.8''$ beam diameter) and also that of LRT ($8''$ beam diameter). There is also a star 0.84 mag fainter than IRS 23 which was likely in the beam of LRT and possibly S87 ($\sim 2.5''$ to the NW). These are probably the worst cases for contamination of the previously published spectra (see Table 1, Paper I), although all the sources in LRT, S87, and Rieke et al. (1989) must have had some contamination. Such contamination can affect the measured absorption strengths of the GC stars and lead to different estimates of stellar spectral types for the GC stars. Of the three stars for which we have analyzed both OSIRIS and S87 re–binned data (IRS 11, 19, and 22), only IRS 11 shows a statistically significant difference in absorption strengths. Therefore, we adopt the OSIRIS values of the absorption strengths for this star. For the remaining two stars (IRS 19 and 22) we adopt an average of the OSIRIS and S87 measurements.

When comparing the present data to previous work, there is only one source upon which there has been disagreement over the most basic spectral characteristics. Krabbe et al. (1991,1995) suggest that IRS 9 is likely a He I emission–line star, or other hot star, based on narrow–band imaging and a spectrum of He I (2.06 μm) emission, but our spectrum clearly shows IRS 9 to be a late type star based on strong CO absorption at 2.3 μm (Figure 1). The Krabbe et al. (1995) spectrum of IRS 9 does not include the 2.3 μm region. Tamblyn et al. (1996) also make the cool star identification based on narrow band imaging. We note that there is small residual Brγ emission in this source after background

subtraction in our spectrum (possibly related to this cool star; see below).

3.2. Comparison to Disk and Bulge Stars

3.2.1. CO & H_2O

Figure 2 shows a comparison of measured CO vs. H_2O for the GC and comparison stars. The bulge giants, disk giants, and LPVs show a correlation between CO and H_2O. A small sample of CO and H_2O data for disk supergiants is also shown in Figure 2. These data show a different relation between CO and H_2O than the giants and LPVs.

CO absorption strength increases with decreasing effective temperature ($T_{\rm eff}$), decreasing gravity, increasing [C/H], and increasing microturbulence (Baldwin et al. 1973; McWilliam & Lambert 1984). This last parameter increases with increasing luminosity (McWilliam & Lambert 1984; McWilliam & Rich 1994). For a star evolving up the giant branch these factors conspire to produce the strong observed correlation of increasing CO absorption strength with increasing $J - K$, where increasing $J - K$ is due to decreasing $T_{\rm eff}$ (McWilliam & Lambert 1984). This correlation holds for giants, on average, to very red $J - K$ but exhibits large scatter in CO for the reddest stars ($J - K \gtrsim 1.2$–1.3 mag). This is true of disk stars (McWilliam & Lambert 1984) and bulge stars (FW87). Much of the increased scatter in both disk and bulge star samples is due to the presence of LPVs in the M giant samples (McWilliam & Lambert 1984; FW87).

H_2O absorption strength also increases with decreasing $T_{\rm eff}$, but decreases with increasing luminosity (Persson et al. 1977; Aaronson et al. 1978; KH; Wallace & Hinkle 1996). A large increase in luminosity (accompanied by a decrease in gravity and increase in microturbulent velocity) leads to significantly higher CO absorption. It is this contrasting luminosity dependence in CO and H_2O which leads to the separation of giants and supergiants in Figure 2.

FW87 and Terndrup et al. (1991) used $(J - K)_\circ$ as a temperature indicator for the BW and disk stars. Because of the much larger interstellar extinction towards the GC, we cannot use the intrinsic colors of the stars as a temperature indicator. We will use the CO strength as a rough indicator of temperature (KH), while keeping in mind CO also depends on luminosity.

The GC and bulge stars have generally stronger H_2O at a given CO strength than the disk stars, and similar H_2O as the LPVs. The H_2O measure is sensitive to the derived A_K. If the derived extinction for a GC star is too high, the H_2O strength in this diagram

is underestimated. We have included in Figure 2 only those GC stars with A_K determined from two or more infrared colors (Paper I).

The A_K values applied here (Paper I) employ the interstellar extinction curve of Mathis (1990). This curve describes a power–law dependence of extinction on the wavelength raised to the -1.7 power (an average of recent determinations, Mathis 1990). Other curves give slightly different powers. The interstellar extinction curve of Rieke & Lebofsky (1985), for example, is well fit by a power−law with exponent equal to -1.6. The law adopted by S87 (van de Hulst No. 15) is represented as a power−law with exponent equal to -1.9. The "flatter" law of Rieke & Lebofsky (1985) would result in A_K about 10 % higher for the same observed colors and assumed intrinsic colors. However, the effect of a higher A_K (to make the derived H_2O absorption smaller) is nearly cancelled by the effect of de–reddening the spectrum with the "flatter" extinction law. Using the Rieke & Lebofsky law to de–redden the spectrum of a GC star and to derive A_K would result in a measured H_2O value only $\sim$ 1.5 % less; i.e, a GC star with H_2O of 12.0 % would shift to $\sim$ 10.5 % if we adopted the Rieke & Lebofsky extinction law. Similarly, if we adopted the same law as S87, the H_2O would be $\sim 1.5\%$ greater.

The CO and H_2O absorption strengths are also expected to change with metallicity. Observations of the integrated light of globular clusters (Aaronson et al. 1978) and of individual stars at fixed V-K in globular clusters and open clusters (Frogel et al. 1983; Houdashelt et al. 1992) show that the CO absorption strength increases with increasing metallicity. The H_2O absorption strength may also increase with increasing metallicity (Aaronson et al. 1978). The strong CO absorption in bulge stars has been attributed to high metallicity (FW87; Terndrup et al. 1991) but McWilliam & Rich (1994) suggest that changes in surface gravity, microturbulence, or the $^{12}C/^{13}C$ ratio could also be important.

3.2.2. CO, "Na," & "Ca"

KH identified Na and Ca as two strong atomic features in the $K−$band for a large range of dwarves, giants, and supergiants. Recent higher spectral resolution data indicates that the situation is more complex for M supergiants and late M giants. The high resolution spectra ($R \geq 45,000$) of M giants and M supergiants presented by Wallace & Hinkle (1996) show that Sc I contributes as much or more to the total equivalent width of both our "Na" and "Ca" measures. Other significant contributors are Ti I, Si I, and V I, to "Na", and Ti I and Fe I to "Ca" (Wallace & Hinkle 1996). Such contamination is confirmed for IRS 7; a high resolution ($R = 40,000$) spectrum of IRS 7 in the "Na" feature shows Sc is likely the largest single atomic contributor to "Na" in our spectrum (Carr et al. 1996a, b). This

strong Sc absorption complicates our interpretation of the "Na" enhancement we observe in IRS 7 relative to disk supergiants (see § 4 below).

The GC stars and the BW stars both appear to have stronger "Na" and "Ca" absorption strengths than the field M giants and M supergiants (Figure 3 and 4). Note that there is more scatter for the "Na" measurement than for "Ca" in Figure 4. It is not clear what causes this difference. It is possible that our local continuum is more affected by the many absorption lines near "Na" than for "Ca" in the GC stars. There is a telluric absorption feature inside our "Na" bandpass; variations in the correction of this feature could lead to differences in derived absorption strength. There may be small residual [Fe III] 2.217 μm emission (Lutz et al. 1993) in some GC star spectra from incomplete background subtraction which could have affected our continuum placement as well. This latter possibility does not affect our conclusion that the "Na" absorption is enhanced. Many of the GC stars with strong "Na" absorption strength are not in regions where diffuse [Fe III] emission is strong, while IRS 20, in a region of strong [Fe III] emission, has a relatively small measured "Na" absorption strength.

Both "atomic" absorption features may also be affected by molecular absorption. There are many lines due to CN identified by Wallace & Hinkle (1996) in our "Na" and "Ca" bandpasses. Higher resolution spectra of IRS 7 (S87; Carr et al. 1996a, b) suggest these are important contributors as well. Model results for giant and supergiant M stars show that a substantial fraction of the total equivalent width of our "Na" and "Ca" equivalent widths could be due to CN absorption (Carr et al. 1996a, b). The effect will also depend on how CN affects the nearby continuum, but it is possible that the atomic features speak as much to CN (and hence CNO processing) as to atomic abundances. Carr et al. (1996a, b) show that CO is weaker in IRS 7 compared to the M2 I α Ori and that CN is stronger. This is consistent with our finding that IRS 7 has weaker CO strength than μ Cep (M2 Ia, see Table 1) but stronger "Na" and "Ca;" see Table 1 and Figures 3 and 4.

4. Discussion

4.1. AGB Stars and Supergiants

The cool GC stars we have observed are more luminous than the tip of the first ascent red giant branch, and therefore must be either AGB stars or supergiant stars. We would like to distinguish between AGB stars and supergiants because each traces different epochs of star formation in the GC (Haller & Rieke 1989; Haller 1992; Krabbe et al. 1995). It is important to separate individual stars between older star formation epochs and more recent

ones since the relative numbers of red and blue supergiants present may be important in constraining starburst models in the GC (Krabbe et al. 1995). LRT and S87 made earlier attempts to distinguish between M giants and supergiants. Here, we re-address this question with our higher angular resolution data (both the spectra presented here, and the photometry in Paper I) and in the context that some of the stars may be AGB stars, in particular, LPVs.

4.1.1. Definitions and Observed Characteristics

In this discussion, we will use the following definitions for AGB stars and M type supergiants taken from Jones et al. (1983). By AGB stars, we mean those intermediate and low mass stars (initial masses, M $\lesssim$9–10 $M_\odot$) with degenerate C/O cores which are producing their luminosity through helium shell and hydrogen shell fusion. The brightest AGB stars are thermally pulsing variables (see Iben & Renzini 1983 and Wood 1990 for reviews of AGB stars) known as Miras and OH/IR stars. Generally, we will call such stars LPVs or AGB stars. AGB stars are generally believed to obey a core-mass vs. luminosity relationship (Paczyński 1970) which limits their maximum luminosity to $M_{\rm bol} = -7.0$ mag. Recent modeling of a 7 $M_\odot$ AGB star suggests slightly higher luminosities ($M_{\rm bol} < -7.2$) are possible (Blöcker & Schönberner 1991). Supergiants are those stars still burning helium (or carbon) in their cores. They will have initial masses generally greater than 10 $M_\odot$. M supergiants can reach bolometric luminosities up to $M_{\rm bol} \lesssim -9.5$ mag, but some have $M_{\rm bol}$ less luminous than -6.0 mag (Humphreys 1978; Figure 5).

LPVs should be regular pulsators with large amplitude variability and long periods. This is strong incentive for continued and more regular variability searches in the GC. While variable, M supergiants do not appear to behave like normal Miras; their variations are typically of smaller amplitude ($\lesssim$0.5 mag at K) and irregular (Harvey et al. 1974; EFH; Jones et al. 1988). Jones et al. (1988) do discuss a small subset of luminous OH/IR stars which may "masquerade" as LPVs, but which are really more massive supergiants. However, these stars are more luminous than the AGB limit. There also exists one optically visible M supergiant (VX Sgr, a strong OH emitter) that may be related to these luminous OH/IR stars (Jones et al. 1988) but in no way appears to be typical of M supergiants or Miras. This star has semi–regular photometric variations (Harvey et al. 1974) and moderate H_2O absorption (Hyland et al. 1972; Jones et al. 1988). To our knowledge, it is the one known star with primarily Mira like characteristics and a supergiant classification (based on spectral characteristics, Lockwood & Wing 1982). Elias et al. (1980) argue that VX Sgr may be similar to the Small Magellanic Cloud (SMC) large amplitude (LA)

variables, i.e., it is in fact an AGB star. We note that the estimated distance to VX Sgr (and hence luminosity) may be quite uncertain, ranging from ~ 250 pc (Celis 1995) to 1500 pc (Lockwood & Wing 1982).

The $H - K$ colors of the Large Magellanic Cloud (LMC), BW M giants, and Sgr I LPVs in Figure 5 have independent measurements of A_K (the A_K is not derived from the observed colors of these stars). Their generally redder colors result from a combination of circumstellar emission, circumstellar extinction, and photospheric colors (Feast et al. 1982; Whitelock et al. 1986; Gaylard et al. 1989; Glass et al. 1995; Zijlstra et al. 1996; see also the discussion on the Sgr I LPVs in Appendix 1). This is assumed to be the case for the much redder IRAS LPVs as well. The reddening vector in Figure 5 suggests that the $H - K$ colors of the IRAS sources might be dominated by circumstellar extinction.

The $K-$band spectra of known Mira variable stars (e.g., o Cet, R Hya, R Cas, and R Leo; Johnson & Méndez 1970; Hyland et al. 1972; Merrill & Stein 1976; Strecker et al. 1978) are characterized by strong CO and H_2O absorption. The H_2O absorption produces a large depression in the continuum which increases in strength toward the blue end of the $K-$band (Figure 1) which cannot be accounted for by interstellar extinction. Narrow–band photometry (Frogel 1983; EFH) and low resolution spectroscopy (Jones et al. 1988) have also clearly associated strong H_2O absorption with LPVs. Miras may also exhibit Brγ emission, the appearance of which may be variable (Johnson & Méndez 1970).

4.1.2. Color–Magnitude Diagram

Figure 5 presents the de–reddened color–magnitude diagram (CMD) for the GC cool stars and compares it to other well–studied populations of supergiants, giants, and LPVs. The GC stars are compared separately to supergiants and AGB stars. Each of the data sets presented in Figure 5 is described in Appendix 1. Here we mention several important points. The GC stars have A_K from Paper I which were determined by assuming intrinsic colors. The A_K may be overestimated ($\lesssim 0.5$ mag) for some GC stars (see the discussion in Appendix 1). The Milky Way supergiants have distances derived from the OB stars in their individual associations.

IRS 7 is the only M star in our spectroscopic sample of the central ~ 5 pc that must be a massive supergiant based on its luminosity. IRS 7 has $M_{\rm bol} = -9.0$ mag ($BC_K = 2.6$ mag for M2 I, EFH; see also Appendix 1). The remainder of the GC stars are below the theoretical upper limit on bolometric luminosity ($M_{\rm bol} = -7.0$) for lower mass AGB stars if we apply the BC_K (2.9–3.2 mag) derived from known LPVs (see Appendix 1).

More than half of GC stars have relatively faint M_K ($\gtrsim-8.0$ mag). These stars have M_K fainter than the faintest supergiant in our comparison sample. However, the Milky Way supergiants do overlap with the LPVs in the range $-10.4 \lesssim M_K \lesssim -8.1$ mag ($-7.8 \lesssim M_{\rm bol} \lesssim -5.5$ mag) and some of the GC stars lie in this range. Clearly M_K cannot be used to unambiguously separate all the GC stars. At this point we can bin the GC stars in Table 2 into three groups based on M_K (assuming, for the moment, they are all M stars): 1.) definite supergiants, IRS 7; 2.) M giant or AGB star, IRS 12S, 20, OSU C1, C2, and C4; 3.) supergiant or luminous AGB star, IRS 1NE, 1SE, 2, 9, 11, 12N, 14NE, 19, 22, 23, 24, 28 and OSU C3. We do not have spectra of the remaining stars in Table 2, but all have $M_K \geq -8.0$ mag and cool star identifications based on published spectra (Krabbe et al. 1995; Figer 1995).

4.2. AGB and LPV Stars in the GC: CO, H$_2$O, & Variability

We have spectra of 13 GC stars which have M_K consistent with either a supergiant or AGB star classification. Seven of these stars (IRS 9, 11, 12N, 14NE, 23, 24, and 28) have strong H$_2$O absorption characteristic of LPVs. IRS 12S, with M_K corresponding to an AGB star, also has strong H$_2$O characteristic of LPVs. These GC stars have CO strength similar to the known LPVs (Miras) in Table 2 with the exception of IRS 23. Inspection of Figure 1 suggests the continuum position of IRS 23 may be affected by additional absorption which depresses it relative to the other stars (also recall that more than one star may contribute to the S87 spectrum of this star).

In addition to having strong H$_2$O like the disk LPVs, IRS 9, 12N, 24, and 28 have recently been identified as photometric variables at K (Haller 1992; Tamura et al. 1994, 1996) and J (IRS 9 and 12N, Paper I). IRS 23 is just below Haller's (1992) three sigma cut–off for variability at K. The spectral characteristics of IRS 9, 12N, and 28 coupled with the photometric variability, strongly support the suggestion by Tamura et al. (1996) that these stars are LPVs like the Miras. A similar case now exists for IRS 24 and most likely IRS 23. Recent searches for variability in the GC (Haller & Rieke 1989; Haller 1992; Tamura et al. 1994, 1996), while ground breaking, are only a first step at characterizing the stellar variability in the GC.

IRS 24 has also been identified with an H$_2$O maser (Levine et al. 1995) and an OH maser (Sjouwerman & van Langevelde 1996). We believe these maser identifications strengthen the case for IRS 24 being an LPV, but see Levine et al. (1995) for a different interpretation. IRS 24 and additional OH masers in our field are discussed in Appendix 2.

Two of the GC stars with M_K implying they are either supergiant or AGB stars (IRS 19 and 22) have strong CO, luminous M_K, and weak H_2O. We conclude that these stars are likely supergiants. We note that Blum et al. (1996, Paper I) find IRS 7 to be variable but with variation (~ 0.3 mag at K) which is consistent with supergiants (Harvey et al. 1974; EFH). It is the combination of weak H_2O, strong CO, and M_K which leads to the supergiant classifications.

This leaves four GC stars (IRS 1SE, 1NE, 2,and OSU C3) with combinations of CO, H_2O, M_K, and variability that do not firmly establish a classification. These four stars may be AGB stars (M7 or later) or K5–M0 supergiants.

The classifications (or lack thereof) for all the GC stars for which we have spectra are summarized in Table 2. Within the uncertainties posed by the ambiguous group, we can now compare the CO and atomic line absorption strengths of the GC stars with similar measures from stars of known populations to further explore the GC star properties.

4.3. Absorption Strengths: GC vs. Bulge and Disk Stars

4.3.1. CO

Figure 2 suggests that the GC stars with supergiant classifications (IRS 7, 19, and 22) all have normal CO strengths for M 0–2 supergiants. The GC stars with AGB or LPV classifications have CO which range from about 14 % to 23 %. On average, the GC AGB/LPV stars appear to have stronger CO than the latest bulge and disk M giants. This is most likely due to the fact that the GC stars represent the coolest, most luminous stars on the AGB; investigation of the CO *abundance* and of the GC population will be better addressed with larger samples of stars which span much earlier spectral types (e.g. FW87). Note that none of the GC AGB/LPVs has CO absorption which is significantly stronger than the CO absorption in the Mira R Cas.

If we assume that the GC stars have CO strengths similar to the disk stars of their respective classes (e.g. supergiant or AGB) we can assign spectral types to them and, hence, obtain an estimate of T_{eff} for each star. We estimate spectral types to the nearest integer sub–type by comparing the GC star CO strength to the representative members of its class in the disk star sample of Table 1. This results in the spectral types shown in Table 1. We adopt the spectral type vs. T_{eff} calibration of Dyck et al. (1996) for the AGB stars. For the LPVs, it does not appear that optical spectral type is well correlated with T_{eff}. Ridgway et al. (1992) showed that o Cet has much lower T_{eff} than non−Mira M giants of the same optical spectral type. Therefore, we estimate T_{eff} in a different way for the LPVs. The

luminosity of LPVs appears to be tightly correlated with mass (Vassiliadis & Wood 1993; Jones et al. 1994). The evolutionary models of Vassiliadis & Wood (1993) suggest masses based on our M_{bol} estimates for the GC stars (see Table 2) which lead to estimates of T_{eff} (from the Vassiliadis & Wood models) that are in close agreement with the derived T_{eff} for o Cet (2300 K) from Ridgway et al. (1992); see the discussion on LPV masses in § 4.4.

We adopt the spectral type vs. T_{eff} calibration of Johnson (1966) for the supergiants; the Johnson scale is consistent with the results of Dyck et al. (1996). The effective temperature of α Ori (M2 I) determined from its angular diameter (Dyck et al. 1992, 1996) is in excellent agreement with the Johnson (1966) value for M2 I (3600 K). The T_{eff} for GC stars is given in Table 2.

By using the above CO (spectral type) vs. T_{eff} calibration we have assumed the GC stars have similar metallicity and CO abundance as the disk stars. This may not be the case. Detailed metallicity and abundance analyses are just now being completed for some GC stars (Carr et al. 1996a, b). If it is found that the GC metallicity scale is much different than the disk stars, we may need to adjust our spectral type and T_{eff} assignments.

4.3.2. "Na" & "Ca"

Figure 3 is strongly affected by T_{eff} and by luminosity. However, the luminosity effect is almost entirely in the CO strength which separates the disk and bulge giants from the disk supergiants. The absorption strength of the "Ca" and "Na" lines is observed to increase with decreasing T_{eff} (KH; Terndrup et al. 1991; Ramírez et al. 1996; all three analyses are affected by the contamination discussed above). The high resolution data of Wallace & Hinkle (1996) also show this trend for the various contributors to "Na" and "Ca" which were identified in § 3. Figure 3 and 4 (disk giants and supergiants) each show a correlation of "Na" and "Ca" with CO where CO now represents, for a fixed luminosity class, a measure of T_{eff}.

Figure 3 suggests that the GC and BW stars have higher "Na" and "Ca" than the disk stars of similar CO strength. For the bulge stars, Terndrup et al. (1991) considered a range of temperatures for both disk and bulge giants and showed that, on average, the "Na" and "Ca" strengths for a given temperature were higher for bulge stars. This effect can be seen in Figures 3 and 4 for the bulge M giants. Consider stars with CO greater than 15 %, which corresponds to the T_{eff} range (actually $J - K \geq 1.00$ mag) for the Terndrup et al. (1991) bulge and disk giants analyzed here. The bulge stars have mean "Na" plus "Ca" which is higher than the disk giants, 12.48 ± 0.67 Å compared to 10.05 ± 0.31 Å.

The enhancement also holds for "Na" and "Ca" individually. The range of M_K for the BW giants suggests some may be on the AGB while others may be first ascent giants. This is likely true of our disk star sample too. Therefore, our comparison could be affected by differences in "Na" and "Ca" absorption resulting from these different evolutionary states.

If we consider the GC AGB/LPV stars in the same range of CO strength as above, we find that "Na" plus "Ca" (12.29 ± 0.82 Å) is also stronger than for the disk stars, and similar to the value for the bulge stars ("Na" and "Ca" are stronger individually too). As for the disk and bulge giant comparison, we caution, that we are primarily comparing disk giants to GC AGB stars since our disk sample only includes one LPV (re–binned high resolution spectrum of o Cet from Wallace & Hinkle 1996). We did not attempt "Na" and "Ca" measurements of the Johnson & Méndez (1970) LPVs due to the lower spectral sampling and poorer signal–to–noise. A larger sample of cool LPVs may show average "Na" and "Ca" which are stronger than the other disk giants in Figure 3.

Terndrup et al. (1991) argued that the enhanced absorption strengths of "Na" and "Ca" in BW reflected enhanced *abundances* relative to disk giants. Their measurements were susceptible to the same contamination problems we discussed above, so it is not clear that the BW stars actually have enhanced Na or Ca, although this is, of course, not ruled out since high resolution spectra have not been obtained in the $K-$band for the BW giants. McWilliam & Rich (1994), in detailed abundance analyses using high resolution optical spectra, found that [Ca/Fe] in a sample of bulge K giants (11 stars) was similar to that expected for disk or halo stars of a given [Fe/H], while Na might be over–abundant in several of their stars.

The GC supergiants show a clear enhancement of "Na" and "Ca" absorption over the disk supergiants, as pointed out for IRS 7 by S87. The mean value of "Na" plus "Ca" for the three GC supergiants is 13.4 ± 1.0 Å. By contrast, the strongest value we find for a disk supergiant is 11.9 Å for SAO 11969 (M3 I), and the remainder of the disk supergiants have "Na" plus "Ca" less than 11.5 Å. Note that this enhancement is seen in "Na" and "Ca" individually as well (Figure 4). IRS 7, clearly a M1–2 supergiant, has "Na" plus "Ca" 2.5 ± 0.7 Å greater than SAO 11969. A high resolution spectrum of IRS 7 suggests that Sc I, which contributes significantly to the "Na" equivalent width, appears enhanced relative to α Ori (M2 I) (Carr et al. 1996a,b; see discussion in § 3). Sc is an iron-peak element whose abundance should follow that of iron (Wheeler, Sneden, & Truran 1989). However, IRS 7 and α Ori exhibit essentially the same [Fe/H] as derived from infrared spectra (the value is nearly solar, Carr et al. 1996a,b). A current lack of laboratory data for the hyperfine splitting in Sc makes it difficult to accurately model its line strengths and derive a precise abundance. An interesting possibility is the enhancement of the Sc abundance by mixing to

the surface the products of mild $s-$processing. Smith & Lambert (1987) predict that the Sc abundance could be significantly enhanced (factor of three) by mild $s-$processed material mixed to the surface in late–type stars. This would require more mixing of processed material than is seen in similar disk stars (e.g. α Ori), assuming the same process occurs in the stellar interiors of disk and GC stars. While helping to solve our Sc abundance problem, we would then need an explanation for the increased mixing in GC stars.

At present, therefore, we do not know whether the strong Sc absorption in IRS 7 (which may also be a significant contributor to the strong "Na" and "Ca" in other GC stars) is due to selective enrichment of Sc (by mild s–processing or some other mechanism) or whether Sc is particularly sensitive to some parameter in the model atmospheres, such as surface gravity or microturbulence, which differs slightly between IRS 7 and α Ori. We plan to make high spectral resolution measurements of the "Na" and "Ca" features to determine the underlying causes of the demonstrated enhancement in absorption strengths. We plan to explore Sc enhancement as well as the effect of the remaining atomic (Ti, V, Si, and Fe) and molecular (CN) lines which contribute to the "Na" and 'Ca" strengths (see § 3).

4.4. Masses and Ages

We may estimate the masses and ages of the GC stars by comparing estimates of their bolometric luminosities and effective temperatures (Table 2) to stellar evolution models. The M1 I classification for IRS 7 (Table 1) is consistent with previous determinations (LRT, S87) and gives $T_{\rm eff} = 3600$ K for our adopted spectral type calibration (§ 4.3.1). The detailed analysis of weaker CO lines from high resolution spectra (Carr et al. 1996a, b) is consistent with this temperature. Taking 3600 K and using the derived value of $M_{\rm bol}$ (-9.0 mag, $BC_K = 2.6$ mag) suggests an initial mass of ~ 20–25 M$_\odot$ and age of 7–9 Myr for the Z $= 0.02$ evolutionary tracks of Schaller et al. (1992). The solar metallicity tracks were chosen based on the Carr et al. (1996a, b) finding that [Fe/H] in IRS 7 is nearly solar. Similarly, the values of $M_{\rm bol}$ and $T_{\rm eff}$ given in Table 2 suggest masses of $12-15$ M$_\odot$ for IRS 19 and $9-12$ M$_\odot$ for IRS 22, again for Schaller et al. (1992) Z $= 0.02$ tracks. Corresponding ages are $\sim 12-18$ Myr and $18-29$ Myr.

The situation for the candidate LPVs (IRS 9, 12N, 23, 24, and 28) is more speculative. Few models exist for evolution near the top of the AGB; such models depend on empirically determined mass–loss rates (Wood 1990). Comparison to the Z $= 0.016$ (largest Z for which models were computed) models of Vassiliadis & Wood (1993) will allow for a rough estimate. Using the BC_K derived from the Sgr I LPVs (3.2 mag, Appendix 1), the GC LPV candidates have $-5.7 \gtrsim M_{\rm bol} \gtrsim -6.5$ mag. The evolutionary models of Vassiliadis & Wood

(1993) predict the relatively narrow mass range of $\sim$ 4–5 M$_\odot$ for (Mira–like) LPVs in this luminosity range. Adopting these masses for the GC LPVs and using their derived M_{bol} gives an estimated T_{eff} of $\sim$ 2600 K, also from the models of Vassiliadis & Wood (1993). This agrees well with the value mentioned above for o Cet, the proto–type Mira. The corresponding ages from the Vassiliadis & Wood models are 120–200 Myr, similar to the 107–190 Myr ages of 4–5 M$_\odot$ stars from the Schaller et al. (1992) models.

The remaining AGB stars in Table 2 have lower M_K and thus M_{bol}. The CO strengths and M_K are consistent with a late M classification, so their BC_K are similar to the BC_K of the Sgr I LPVs (FW87, Glass et al. 1995). For simplicity, we use the same BC_K (3.2 mag, Appendix 1). We estimate, by comparison to the Schaller et al. (1993) tracks, that the remaining AGB stars have maximum initial masses of $\sim 3 - 4$ M$_\odot$, corresponding to minimum ages of $\sim 190 - 440$ Myr. The tracks of Vassiliadis & Wood (1993) for AGB stars suggest that the brightest GC AGB stars, IRS 11 and 14NE, must have minimum initial masses ~ 2 M$_\odot$ in order to reach their observed luminosities. This corresponds to maximum ages of ~ 1.6 Gyr. Similarly, IRS 12S, OSU C1, C2, and C4 have minimum initial masses of ~ 1 M$_\odot$ and maximum ages of ~ 12 Gyr. Extrapolating the results of Vassiliadis & Wood (1993) to the luminosity of IRS 20 suggests a minimum mass of about 0.8 M$_\odot$ for this star. The corresponding age from the Schaller et al. (1993) Z = 0.02 tracks is ~ 25 Gyr. Since this is longer than the age of the universe (Sandage 1988; Freedman et al. 1994), IRS 20 is likely an AGB star which is more massive than 0.8 M$_\odot$ but which is still evolving up the AGB and has not reached its maximum luminosity on the AGB yet.

We have been unable to distinguish between AGB stars or supergiants for four of the GC stars: IRS 1NE, 1SE, 2, and OSU C3. If these stars are AGB stars they would have M < 3–5 M$_\odot$ and age > 120–440 Myr. The minimum masses for this case would be approximately 1,2,2, and 4 M$_\odot$ for IRS 1SE, 1NE, OSU C3, and IRS 2, respectively, with corresponding maximum age of $\sim 200 - 12000$ Myr. However, using BC_K and T_{eff} as for the supergiants above, IRS 1NE, 1SE and OSU C3 could have initial masses as high as 9 M$_\odot$ and ages ~ 29 Myr. Similarly, we would estimate M ~ 12 M$_\odot$ and age ~ 16 Myr for IRS 2 if it is a supergiant.

The estimates of M_{bol}, T_{eff}, mass, and age are summarized in Table 2. The difference in age for these luminous M stars suggests that there have been multiple, recent epochs of star formation in the GC. Star formation models have been computed in the GC (Tamblyn & Rieke 1993; Krabbe et al. 1995). These models rule out "continuous" star formation on the grounds that this mode would produce many more red supergiants relative to the known blue supergiants (i.e. the emission–line stars; see § 1). A picture of star formation in the GC which is consistent with the results summarized in Table 2 and the aforementioned

model results is one in which small bursts have occurred in a quasi–periodic fashion at different locations leading to the mix of luminous stars we presently observe in the central $\sim 4-5$ pc. In this case, IRS 7 would be one of the older stars in the 3–7 Myr burst model of Krabbe et al. (1995) which also accounts for the large number of massive emission–line stars in the central parsec. The other GC stars result from earlier star formation epochs, $\sim 10-30$ Myr and $\gtrsim 100$ Myr ago.

5. SUMMARY

We have compared the M_K, CO absorption, and H_2O absorption for a sample of GC stars to the same quantities derived from photometry and $K-$band spectra of known populations of supergiants, giants, and LPVs. The GC stars span the brightest five magnitudes in the observed $K-$band luminosity function presented by Blum et al. (1996, Paper I). Of all the bright stars in the GC identified as cool, based on $K-$band spectra, only IRS 7 must be a younger supergiant. The remainder are consistent with less massive M giants and LPVs. Based on bolometric corrections from the known populations of LPVs, none of the GC stars (except IRS 7) has $M_{\rm bol}$ which exceeds the theoretical limit of -7.0 mag for AGB stars. Some GC stars do have luminosities which overlap with the less luminous Milky Way supergiants. Two of these (IRS 19 and 22) exhibit CO and H_2O absorption characteristic of supergiants; we therefore classify them as such. All but four of the remaining GC stars for which we have spectra are classified as AGB/LPV stars. Classification for four stars remains ambiguous between AGB and supergiant.

The coolest, most luminous AGB stars are LPVs. Our $K-$band spectra of four photometric variables in the GC (IRS 9, 12N, 24, and 28) and one possible variable (IRS 23) show extreme H_2O absorption which is remarkably similar to that exhibited by known galactic LPVs. Based on this similarity and variability, we conclude that they are very likely LPVs, as suggested for IRS 9, 12N, and 28 by Tamura et al. (1996). A similar conclusion was reached by Sjouwerman & van Langevelde (1996) for IRS 24 based on its OH maser characteristics. Evolutionary models suggest these LPVs had initial masses of $\sim 4-5$ $M_\odot$ and are roughly 100–200 Myr old. This is in contrast to the M1–2 supergiant, IRS 7, for which we estimate an initial mass of 20–25 $M_\odot$ and age of 7–9 Myr. The other GC supergiants may have masses in the range 9–15 $M_\odot$ and ages of 12–29 Myr. We believe the luminous, cool stars in the GC are tracing multiple epochs of star formation, perhaps as quasi–periodic bursts, over the last 7–100 Myr.

Our analysis of the spectra for the cool stars in the GC results in absorption strengths of CO, H_2O, "Na", and "Ca." The atomic measurements of "Na" and "Ca" from our low

spectral resolution data are shown to be severely contaminated by other atomic species including Si, Fe, Ti, Sc, and V and also molecular lines of CN. The measurements for the four stars we classify as supergiants show a clear enhancement in "Na" and "Ca" over disk supergiants. This includes the well–known GC supergiant IRS 7 which shows a significant enhancement relative to the disk supergiant in our sample with the largest "Na" and "Ca" strength. One component contributing to the enhancement in IRS 7 is Sc, an iron–peak element which may be enhanced by mild s–processing. In general, the cause of the enhancement remains a puzzle which we plan to investigate further with high spectral resolution observations.

The AGB/LPV stars in the GC also have enhanced "Na" and "Ca" relative to disk giant stars. The measured "Na" and "Ca" strengths in these GC stars are similar to those found in the coolest bulge M giants. Temperature and luminosity effects make it difficult to determine abundance effects in the GC AGB stars relative to disk stars. We plan to make additional high resolution measurements of AGB/LPV GC stars, like the supergiants, in order to better understand the underlying causes of the enhanced "Na" and "Ca" absorption strengths.

6.   Appendix 1

The photometry used in constructing Figure 5 is described herein.

Galactic Center cool stars. The GC photometry is described in Paper I. Here, we adopt a distance to the GC of 8 kpc (Reid 1993). The extinction (A_K) was derived by

assuming intrinsic colors for the GC stars, so we cannot distinguish the spectral type of the GC stars by color. However, the spectra in Figure 1 identify all the GC stars as M stars based on their strong CO absorption (and/or H_2O; e.g, IRS 23). IRS 1SE and 2 may be an exceptions, but they would have to be a late K supergiants if not an M giants (compare HR 8726 in Table 1). The intrinsic colors for normal M giants and supergiants do not vary a great deal; therefore, adopting a set of intrinsic colors on the giant branch leads to estimates for A_K which are relatively accurate. In Paper I, stars with measured $J - H$ and $H - K$ had adopted values of 0.7 mag and 0.3 mag, respectively, for these colors from FW87 (these are similar to the intrinsic colors of M supergiants, EFH). If only $H - K$ was available, the star was de–reddened to a mean relation which resulted in a similar $H - K$. It is unlikely that any of the GC stars has intrinsic colors substantially more blue than these. Therefore, it is unlikely that we have substantially underestimated the intrinsic luminosity of any GC star in Figure 5. For example, an $H - K$ of 0.2 mag, instead of 0.3 mag, would result in A_K and the K luminosity being underestimated by 0.16 mag.

What if some of the GC stars are LPVs, not normal giants or supergiants? As we will see below, LPVs may have redder colors than we adopted in Paper I for the GC stars. This means any GC star which is actually an LPV is likely to have had its intrinsic luminosity overestimated. The $J - H$ and $H - K$ colors of the reddest LPVs in Glass et al. (1995) are 1.10 and 0.61 mag, respectively. If these colors were adopted for the GC LPV candidates (Table 2), the resulting A_K would be 0.45 mag less and M_K would therefore be 0.45 mag fainter. Additionally, the color−color diagram for stars in the GC field (Paper I) suggests a minimum A_K of $\gtrsim 2.0$ mag for any star likely to be physically located near the GC. This value can be used to estimate a minimum luminosity for any GC star (Table 2).

We have plotted in Figure 5 all stars in the GC for which we have obtained at least H and K photometry and for which cool star identifications exist (Paper I). The absolute K magnitudes ($R_\circ = 8$ kpc) and A_K from Paper I are listed in Table 2.

Milky Way and LMC M supergiants. The supergiant data were drawn from the sample of EFH which they used to derive intrinsic colors and bolometric corrections for Milky Way and LMC supergiants. The Milky Way data shown in Figure 5 are the subset of stars from the EFH sample with distances determined by Humphreys (1978) from the OB stars in individual associations. The majority of Milky Way supergiants plotted in Figure 5 are luminosity class Iab (22 stars), but luminosity classes range from Ib (four stars) to Ia (five stars). The 31 confirmed LMC supergiants in EFH with infrared photometry are nearly equally split among luminosity classes Ia (15 stars) and Iab (11 stars) with the remainder having no luminosity class assigned. EFH found that the bolometric correction for Milky Way supergiants is nearly constant among sub–types and that this value is quite similar to

those determined for supergiants in the LMC and SMC which are well known to have lower metallicity than Milky Way stars (e.g, Dufour 1986 and references therein). The full range of BC_K for Milky Way, LMC, and SMC M supergiants is 2.5–2.8 mag.

The $H - K$ and BC_K of M supergiants which we have adopted (EFH) are slightly smaller than the values given by Lee (1970). Lee's $H - K$ are up to 0.10 mag more red for type Ia supergiants and the BC_K derived from Lee's $V - K$ and BC_V are up to ~ 0.3 mag larger; i.e, for the same $M_{\rm bol}$, we would compute M_K up to 0.3 mag brighter. This would tend to separate the supergiants more from other stars in Figure 5.

Milky Way M giants. The Milky Way M giants are plotted as the solid line in Figure 5 which rises to $M_K = -8.0$ mag. The line was obtained by using the relationship for absolute visual magnitude vs. MK spectral type derived by Thé et al. (1990) in combination with the $V - K$ and $H - K$ colors of Lee (1970) and Frogel et al. (1978). The adopted $V - K$ are similar to the values given by Johnson (1966). The colors for type M7 III are an average of those for BK Vir and SW Vir (Frogel et al. 1978; Wisse 1981; Mermilliod 1987).

Sgr I LPVs. These are Mira variables observed in the optical window Sgr I ($l, b =1.5°$, $-2.7°$) by Glass et al. (1995). A distance of 8 kpc to the GC (Reid 1993) was assumed to derive absolute K magnitudes. The data were de–reddened by ~ 0.2 mag at K (Glass et al. 1995). Differences between the two systems at H and K are unimportant for this comparison: $\lesssim 5$ % at K and $\lesssim 1$ % at $H - K$ (see the transformation from SAAO to CTIO, Glass et al. 1995 and Carter 1990), so the Sgr I photometry is not transformed on to the same system as EFH (CIT/CTIO). Glass et al. show that these stars are significantly redder than solar neighborhood M giants and known solar neighborhood Miras in $H - K$. The redder colors are due to photospheric effects and/or circumstellar dust (Feast et al. 1982; Whitelock et al. 1986; Gaylard et al. 19 89; Glass et al. 1995; Zijlstra et al. 1996) Note that estimated extinction was determined independent of the Sgr I Miras in Figure 5. We have included stars in Figure 5 from the list of Glass et al. (1995) with $M_K \leq -7.0$. For clarity, we have plotted one third of the stars in the actual sample. Glass et al. derive bolometric magnitudes for these stars from which we find $BC_K = 3.24 \pm 0.15$ mag for all the stars in their sample with $M_K \leq -7.0$.

Baade's window M giants. The BW M giants are taken from the list in FW87. This includes variable stars as indicated by FW87 and the LPVs of Lloyd Evans (1976) which have infrared photometry from FW87 and Glass et al. (1982). Like the Sgr I LPVs, the BW stars have estimated A_K which is small (~ 0.14 mag) and determined independently of the M giants themselves.

LMC optical LPVs. This is an analogous data set to the Sgr I field, but for the

LMC. We have adopted a distance of 46.8 kpc (Reid and Strugnell 1986). The colors and magnitudes are taken from the large amplitude variable list of Hughes & Wood (1990). We plot in Figure 5 M stars with $M_K \lesssim -6.9$ mag; for clarity, not all the stars are plotted. These stars are identified as Miras by Hughes & Wood and were discovered optically. Note that this subset of LMC Miras reaches higher luminosities than those in the Galactic bulge (Sgr I field). This is presumably due to their higher mass (and hence younger age). We also expect slightly more luminous M_{bol} for the lower metallicity LMC stars (Vassiliadis & Wood 1993), but this difference may be compensated for by the different BC_K for the two populations. Using the bolometric and K magnitudes tabulated in Hughes & Wood (1990), we find $BC_K = 2.94 \pm 0.12$ for stars with M spectral types and $M_K \leq 6.9$ mag.

LMC IRAS LPVs and supergiants. These are IRAS selected sources in the LMC taken from Wood et al. (1992) and Zijlstra et al. (1996); they generally have no optical counterparts. Zijlstra et al. identify candidate AGB stars and supergiants. The LPV stars might be similar to optically discovered Miras but with thicker circumstellar dust shells. Zijlstra et al. classified IRAS sources as supergiants based primarily on a luminosity criterion, but a small number were classified based on color and/or small amplitude variability at K. We plot the IRAS sources here mainly to emphasize the possible range of colors for LPVs. The very red colors for this set are due to circumstellar dust shells. The red color is due to a combination of local extinction in the shell, excess emission from the dust in the shell, and photospheric effects in the underlying star.

SMC LA LPVs. EFH identified a small group of luminous, large amplitude (LA) variables in the SMC among their larger sample of supergiants. Based on the photometric variability of these stars and their very large H_2O absorption (as determined by narrow–band photometry) EFH classified these variables as lower mass AGB stars, rather than supergiants (see also Frogel 1983 and Wood et al. 1983).

7. Appendix 2

Here we include a brief discussion of the infrared counterparts to the known OH and H_2O masers within our GC field.

Levine et al. (1995) reported detection of an H_2O maser within our field which they associated with the bright infrared source which we define as IRS 24 (Paper I). Levine et al. interpreted IRS 24 as a late type M supergiant based on a qualitative analysis of its spectrum, H_2O maser emission, and derived M_K from the analysis of H, K, and narrow–band L magnitudes. Their observed H and K magnitudes are within 0.04 mag

of the values we reported in Paper I. However, their adopted extinction law (Rieke et al. 1989) results in a de–reddened K magnitude which is ~ 0.9 mag brighter than the value we derive (Table 2). Most of the difference comes from the adopted A_L/A_K in the Rieke et al. extinction law which is larger than the value in the Mathis (1990) law which we have adopted.

D. Levine and D. Figer have kindly given us a copy of their IRS 24 spectrum which we have analyzed along with our other GC spectra (Figure 1, Table 1). This source has strong CO and H_2O absorption in its $K-$band spectrum (Levine et al. 1995; Table 1). We find that the derived CO and H_2O strengths (Table 2) for IRS 24 are more consistent with an LPV classification than a late type supergiant (Figure 2). Sjouwerman & van Langevelde (1996) recently detected 1612 MHz OH emission associated with IRS 24 and concluded that it is most likely an intermediate mass LPV star (i.e., it is Mira–like). We believe the infrared colors, K magnitude and variability, derived A_K, the infrared spectrum, and H_2O and OH maser emission are most consistent with the LPV classification. Although, note that the mass and age we derive for IRS 24 (Table 2) correspond to a somewhat younger, and more luminous star than suggested by Sjouwerman & van Langevelde (1996).

There are four other 1612 MHz OH/IR stars within our field from the lists of Winnberg et al. (1985) and Lindqvist et al. (1992). Three of the four OH/IR stars in our field have infrared counterparts with $K > 10.5$ mag. We have no spectra or variability information for them.

The fourth OH/IR star is of particular interest. This is star OH359.95–0.05 (Winnberg et al. 1985) or OH359.946–0.047 (Lindqvist et al. 1992). This source is within $1''$ of source IRS 10* which was identified as a photometric variable by Tamura et al. (1996). IRS 10* was identified by Blum et al. (1996, Paper I) as a very red $K-$band source ($K = 10.75$ mag) which was not detected at H or J but which was detected at L. Blum et al. (1996) called this source IRS 10EL. The position of IRS 10* is between IRS 10E and 10W (Tamura et al. 1996; Blum et al. 1996); the OH/IR star is also positionally coincident with IRS 10E within the uncertainties ($\sim 1''$ using the position for IRS 7 from Tollestrup et al. 1989, the position for OH359.946–0.047 from Lindqvist et al. 1992, the associated uncertainties for both, and the offsets in Paper I). We believe the very red $K - L$ color of IRS 10*, as reported in Paper I, strongly enhances the suggestion by Tamura et al. (1996) that it is the near-infrared counter–part to OH359.946–0.047 and therefore, a luminous LPV.

REFERENCES

Aaronson, M., Frogel, J. A., & Persson, S. E 1978, ApJ, 220, 442

Allen, D. A., Hyland, A. R., & Hillier, D. J. 1990, MNRAS, 244, 706

Baldwin, J. R., Frogel, J. A., & Persson, S. E. 1973, ApJ, 184, 427

Blöcker, T. & Shönberner, D. 1991, A&A, 244, L43

Blum, R. D., Sellgren, K., & DePoy, D. L. 1995a, ApJ, 440, L17

Blum, R. D., DePoy, D. L., & Sellgren, K., 1995b, ApJ, 441, 603

Blum, R. D., Sellgren, K., & DePoy, D. L. 1996, ApJ, in press (Paper I)

Carr, J. S., Sellgren, K., & Balachandran, S. 1996a, in *9th Cambridge Workshop on Cool Stars, Stellar Systems, and the Sun,* ed. R. Pallavicini, in press

Carr, J. S., Sellgren, K., & Balachandran, S. 1996b, in the *4th ESO/CTIO Workshop on the Galactic Center*, eds. R. Gredel & R. Schommer, ASP conf. ser., in press

Carter, B. S. 1990, MNRAS, 242, 1

Celis, L. 1995, ApJS, 98, 701

DePoy, D. L., Atwood, B., Byard, P., Frogel, J. A., & O'Brien, T. 1993, in SPIE 1946, "Infrared Detectors and Instrumentation," pg 667

Dufour, R. J. 1986, PASP, 98, 1025

Dyck, H. M, Benson, J. A., Ridgway, S. T., & Dixon, D. J. 1992, AJ, 104, 1992

Dyck, H. M, Benson, J. A., van Belle, G. T., & Ridgway, S. T. 1992, AJ, 111, 1996

Elias, J. H., Frogel, J. A., & Humphreys, R. M. 1980, ApJ, L13

Elias, J. H., Frogel, J. A., & Humphreys, R. M. 1985, ApJS, 57, 91 (EFH)

Feast, M. W., Robertson, B. S. C., Catchpole, R. M., Evans, T. L., Glass, I. S., Carter, B. S. 1982, MNRAS, 201, 439

Figer, D. F. 1995, Ph.D. Dissertation, University of California at Los Angeles

Freedman, W. L., et al. 1994, Nature, 371, 757

Forrest, W. J., Shure, M. A., Pipher, J. L., & Woodward, C. E. 1987, in *The Galactic Center*, ed. Backer, D. C., AIP, New York, p. 153

Frogel, J. A., Persson, S. E., Aaronson, M., & Matthews, K. 1978 ApJ, 220, 75

Frogel, J. A., Cohen, J. A., & Persson, S. E. 1983, ApJ, 275 773

Frogel, J. A. 1983, ApJ, 272, 116

Frogel, J. A. & Whitford, A.E. 1987, ApJ, 320, 199 (FW87)

Gaylard, M. J., West, M. E., Whitelock, P. A., Cohen, R. J. 1989, MNRAS, 236, 247

Glass, I. S. & Feast, M. W. 1982, MNRAS, 198, 199

Glass, I. S., Whitelock, P. A., Catchpole, R. M., & Feast, M. W. 1995, MNRAS, 273, 383

Haller, J. W. & Rieke, M. J. 1989, In *The Center of the Galaxy*, IAU Symp. 136, ed. M. Morris (Dordrecht: Kluwer), 487

Haller, J. 1992, Ph.D. Dissertation, University of Arizona, Tucson

Hanson, M. M., Conti, P. S., & Rieke, M. J. 1996, ApJS, in press

Harvey, P. M., Bechis, K. B., Wilson, W. J., & Ball, J. A. 1974, ApJS, 27, 331

Hinkle, K., Wallace, L., & Livingston, W. 1995, PASP, 107, 1042

Hoffleit, D., 1982, The Bright Star Catalog, Yale University Press, New Haven

Houdashelt, M. L., Frogel, J. A., & Cohen, J. A. 1992, AJ, 103, 163

Hughes, S. M. G. & Wood, P. R. 1990, AJ, 99, 784

Humphreys, R. M. 1978, ApJS, 38, 309

Hyland, A. R., Becklin, E. E., Frogel, J. A., & Neugebauer, G. 1972, A&A, 16, 204

Iben, I. & Renzini, A. 1983, ARA&A, 21, 271

Johnson, H. 1966, ARA&A, 4, 193

Johnson, H. L. & Méndez, M. E. 1970, AJ, 75, 785

Jones, T. J., Hyland, A. R., Wood, P. R., & Gatley, I. 1983, ApJ, 273, 669

Jones, T. J., Hyland, A. R., Fix, J. D., Cobb, M. L. 1988, AJ, 95, 158

Jones, T. J., McGregor, P. J., Gehrz, R. D., & Lawrence, G. F. 1994, AJ, 107, 1111

Kleinmann, S.G. & Hall, D.N.B. 1986, ApJS, 62, 501 (KH)

Krabbe, A., Genzel, R., Drapatz, S., & Rotaciuc, V. 1991, ApJ, 382, L19

Krabbe, A., et al. 1995, ApJ, 447, L95

Lebofsky, M. J., Rieke, G. H., & Tokunaga, A. T. 1982, ApJ, 263, 736 (LRT)

Lee, T. A. 1970, ApJ, 162, 217

Levine, D., Figer, D. F., Morris, M., & McLean, I. S. 1995, ApJ, 447, 101

Libonate, S., Pipher, J. L., Forrest, W. J., & Ashby, M. L. N. 1995, ApJ, 439, 202

Lindqvist, M., Habing, H. J., Winnberg, A., & Matthews, H. E. 1992, A&AS, 92, 43

Lockwood, G. W. & Wing, R. F. 1982, MNRAS, 198, 385

Lloyd Evans, T. 1976, MNRAS, 174, 169

Lutz, D., Krabbe, A., & Genzel, R. 1993, ApJ, 418, 244

Mathis, J.S. 1990, ARA&A28, 37

McWilliam, A. & Lambert, D. 1984, PASP, 96, 882

McWilliam, A. & Rich, R. M. 1994, ApJS, 91, 749

Merrill, K. M. & Stein, W. A. 1976, PASP, 88, 285

Mermilliod, J. C. 1987, A&AS, 71, 413

Morris, M. 1993, ApJ, 408, 496

Nicolet, B. 1978, A&AS, 34, 1

Persson, S. E, Aaronson, M., & Frogel, J. A. 1977, AJ, 82, 729

Paczyński, B. 1970, Acta Astron., 20, 47

Ramírez, S. V., DePoy, D. L., Frogel, J. A., & Sellgren, K. 1996, in preparation

Reid, M. J. 1993, ARA&A, 31, 345

Reid, I. N. & Strugnell, P. R. 1986, MNRAS, 221, 887

Rieke, G. H. & Lebofsky, M. J. 1985, ApJ, 288, 618

Rieke, G. H., Rieke, M. J., & Paul A. E. 1989, ApJ, 336, 752

Ridgway, S. T., Joyce, R. R., White, N. T., & Wing, R. F. 1980, ApJ, 235, 126

Ridgway, S. T., Benson, J. A., Dyck, H. M., Townsley, L. K., & Hermann, R. A. 1992, AJ, 104, 2224

Sandage, A. 1988, ARA&A, 26, 561

Schaller, G., Schaerer, D., Meynet, G., & Maeder, A. 1992, A&AS, 96, 269

Sellgren, K., Hall, D.N.B., Kleinmann, S.G., & Scoville, N.Z. 1987, ApJ, 317, 881 (S87)

Sjouwerman, L. O. & van Langevelde, H. J. 1996, ApJ, 461, L41

Smith, V. V. & Lambert, D. L. 1987, MNRAS, 226, 563

Strecker, D. W., Erickson, E. F., & Witteborn, F. C. 1978, AJ, 83, 26

Tamblyn, P. & Rieke, G. H. 1993, ApJ, 414, 573

Tamblyn, P., Rieke, G. H., Hanson, M. M., Close, L. M., McCarthy, D. W., Jr., & Rieke, M. J. 1996, ApJ, 456, 206

Tamura, M., Werner, M. W., Becklin, E. E., & Phinney, E. S. 1994, in *Infrared Astronomy with Arrays: The Next Generation,* ed. I. McLean, Kluwer Academic Publishers, Dordrecht, p. 117

Tamura, M., Werner, M. W., Becklin, E. E., & Phinney, E. S. 1996, ApJ, in press

Terndrup, D. M., Frogel, J. A., & Whitford, A. E. 1990, ApJ, 357, 453

Terndrup, D. M., Frogel, J. A., & Whitford, A. E. 1991, ApJ, 378, 742

Tollestrup, E. V., Capps, R. W., & Becklin, E. E. 1989, AJ, 98, 204

Thé, P. S., Thomas, D., Christensen, C. G., & Westerlund, B. E. 1990, PASP, 102, 565

Vassiliadis, E. & Wood, P. R. 1993, ApJ, 413, 641

Wallace, L. & Hinkle, K. 1996, ApJS, in press

Wheeler, J. C., Sneden, C., & Truran, J. W. 1989, ARA&A, 27, 279

Whitelock, P., Feast, M., Catchpole, R. 1986, MNRAS, 222, 1

Winnberg, A., Baud, B., Matthews, H. E., Habing, H. J., & Olnon, F. M. 1985, ApJ, 291, L45

Wisse, P. N. J. 1981, A&AS, 44, 273

Wood, P. R., Bessell, M. S., & Fox, M. W. 1983, ApJ, 272, 99

Wood, P. R. 1990, in *From Miras to Planetary Nebulae: Which Path for Stellar Evolution?*, eds. M. O. Mennessier & A. Omont, Yvette Cedex: Editions Frontières, p. 67

Wood, P. R., Whiteoak, J. B., Hughes, S. M. G., Bessell, M. S., Gardner, F. F., & Hyland, A. R. 1992, ApJ, 397, 552

Zijlstra, A. A., Loup, C., Waters, L. B. F. M., Whitelock, P. A., van Loon, J. T., & Guglielmo, F., 1996, MNRAS, 279, 32

Fig. 1.— Spectra of cool Galactic center (GC) stars, obtained using OSIRIS with $\lambda/\Delta\lambda = 570$. All spectra have been corrected for interstellar reddening and are presented as a normalized ratio of the GC star to an A or B star. Note the strong absorption longward of 2.3 μm due to CO in all the stars and strong absorption due to H_2O shortward of 2.2 μm in some of the stars. Emission lines are likely due to incomplete subtraction of the diffuse nebular emission in the GC for some stars (e.g. IRS 2) but may be associated with other cool stars (e.g. IRS 9); see text. The spectra labeled M0 III, M3 III, and M7 III are examples of our spectral data set for disk M giants with optically determined spectral types. IRS 24 is from Levine et al. (1995); R Cas is from Johnson & Méndez (1970). We also show high resolution spectra, after re–binning to $\lambda/\Delta\lambda = 570$, of IRS 7 and IRS 23 from Sellgren et al. (1987) and of μ Cep (M2 Ia) from Kleinmann & Hall (1986).

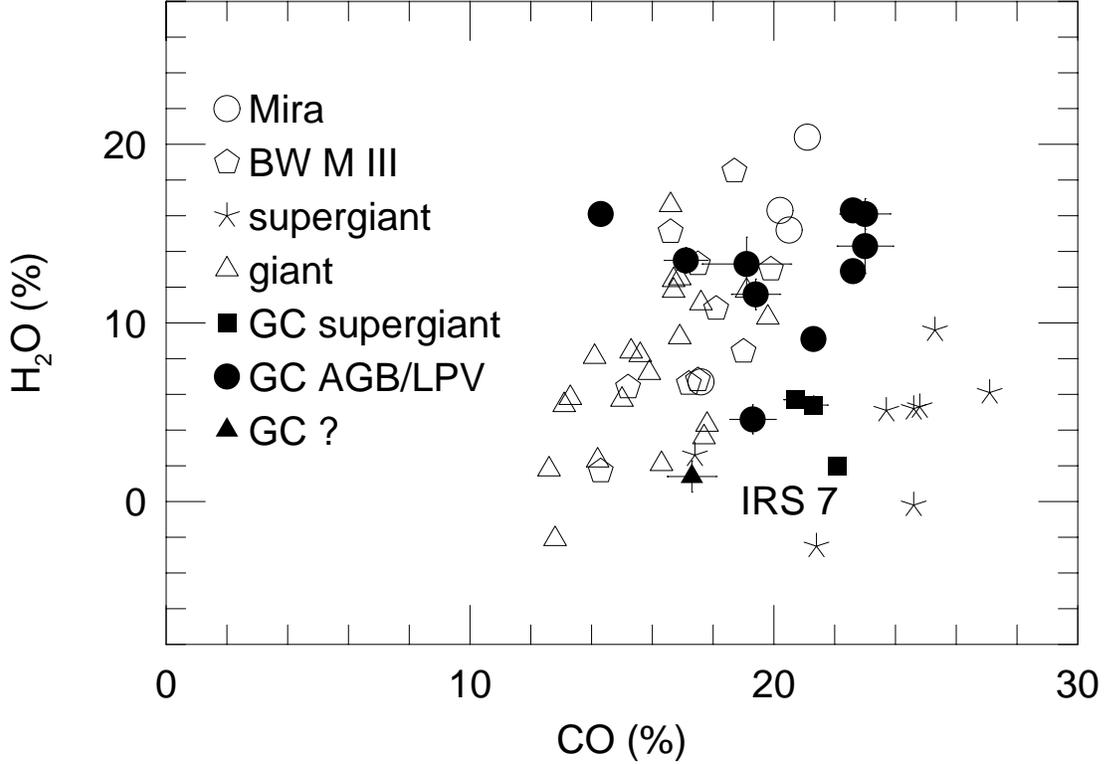Normalized Dereddened Ratio

Wavelength (μm)
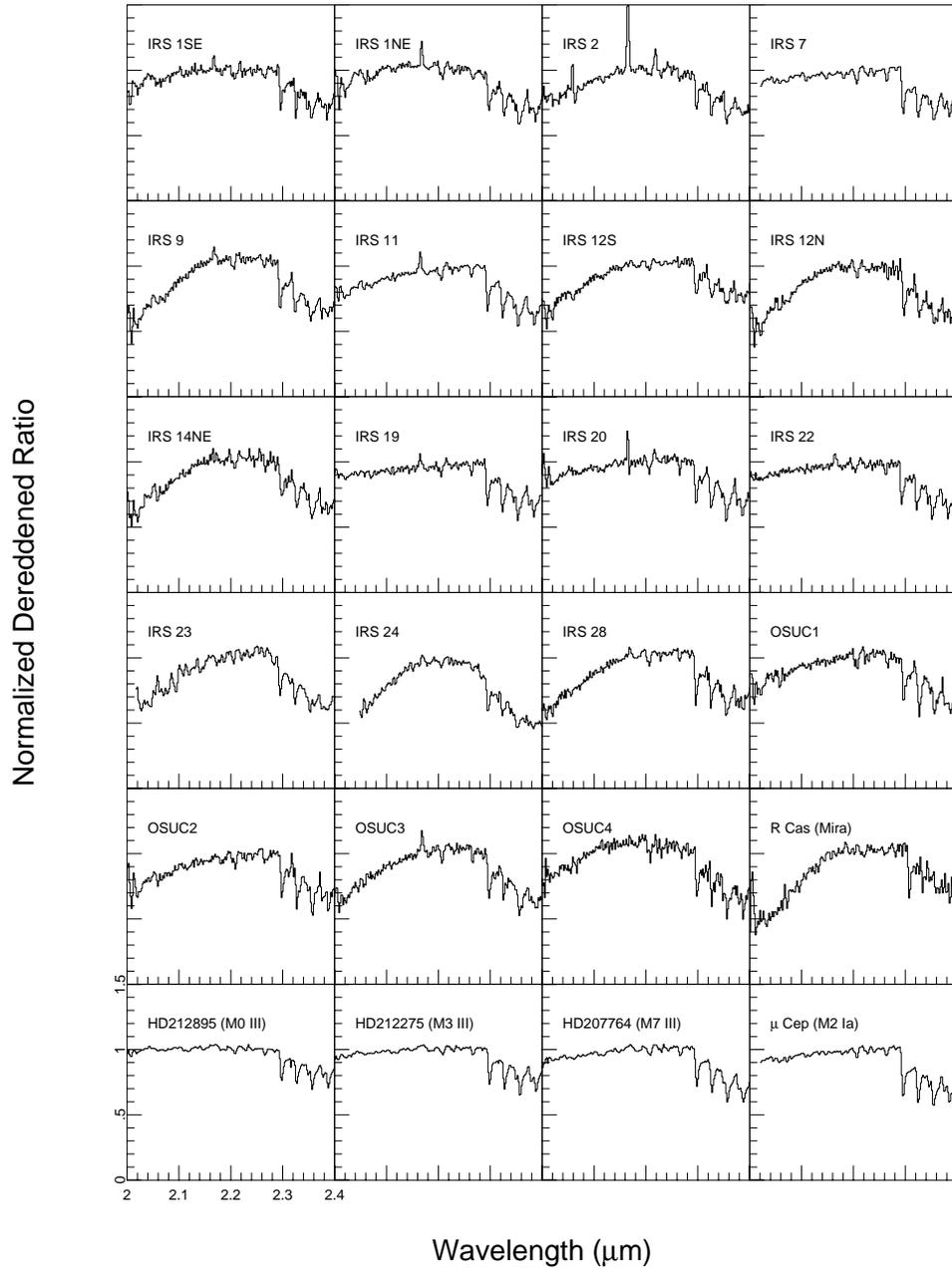
Fig. 2.— Measured H_2O vs. CO strength for Galactic center (GC) stars (*filled symbols*) disk giants (*open triangles*), disk supergiants (*asterisks*), Baade's window (BW) M giants (*open pentagons*), and disk Miras (*open circles*). The GC stars are identified as supergiants (*filled squares*), asymptotic giant branch (AGB) stars or long period variables (LPVs) (*filled circles*), and ambiguous (*filled triangles*). The GC data are from the present work, Sellgren et al. (1987) and Levine et al. (1995). Only GC stars with A_K determined from two infrared colors are plotted. The disk stars are from the present work, Terndrup et al. (1991) and Kleinmann & Hall (1986). The Mira variables (or long period variables, LPVs) are from Johnson & Méndez (1970). The BW M giants are from Terndrup et al. (1991). The error bars reflect measurement uncertainty (Table 1) and uncertainty in A_K (uncertainties listed in Table 2). The large value of H_2O for some of the GC stars suggests they are LPVs; see text.
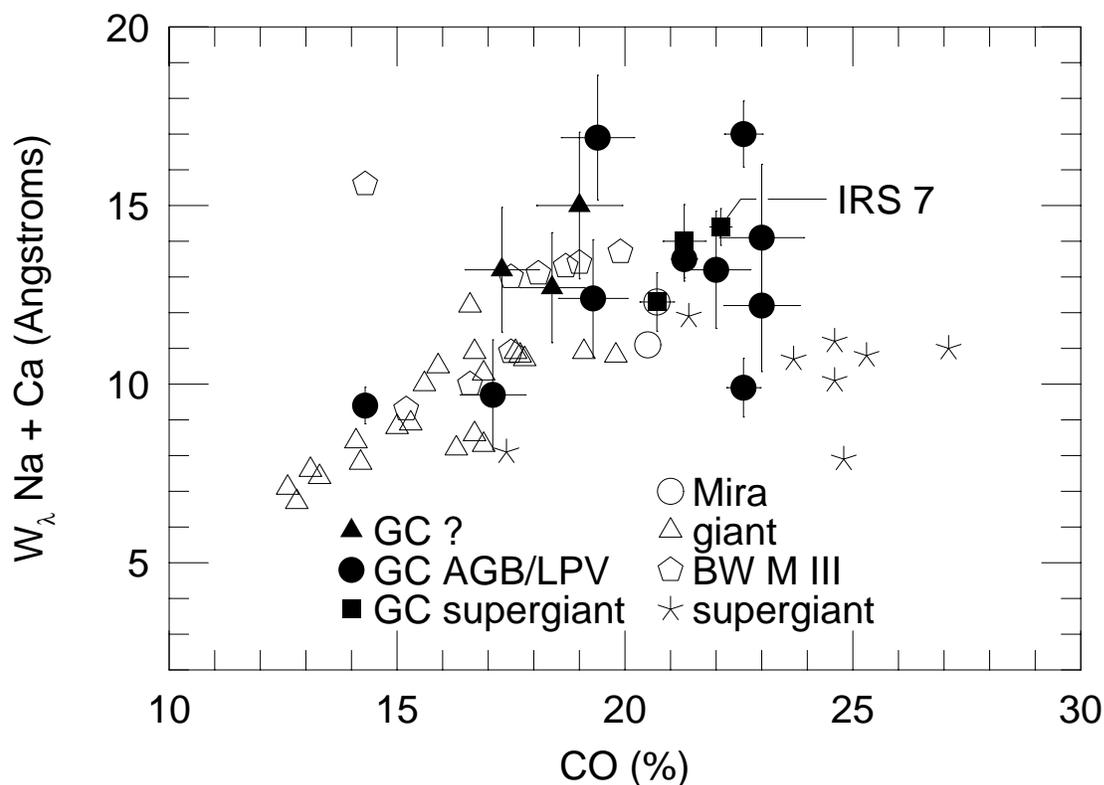
Fig. 3.— Sum of measured "Na" and "Ca" equivalent widths vs. CO strength. Symbols are the same as for Figure 2. Competing effects of abundance, luminosity, and effective temperature all play a role in this diagram. Galactic center (GC) stars identified as asymptotic giant branch (AGB) or long period variables (LPVs) have similar "Na" plus "Ca" absorption as bulge giants and are enhanced relative to disk giants. GC stars identified as supergiants (e.g. IRS 7) have significantly higher "Na" plus "Ca" than disk supergiants.
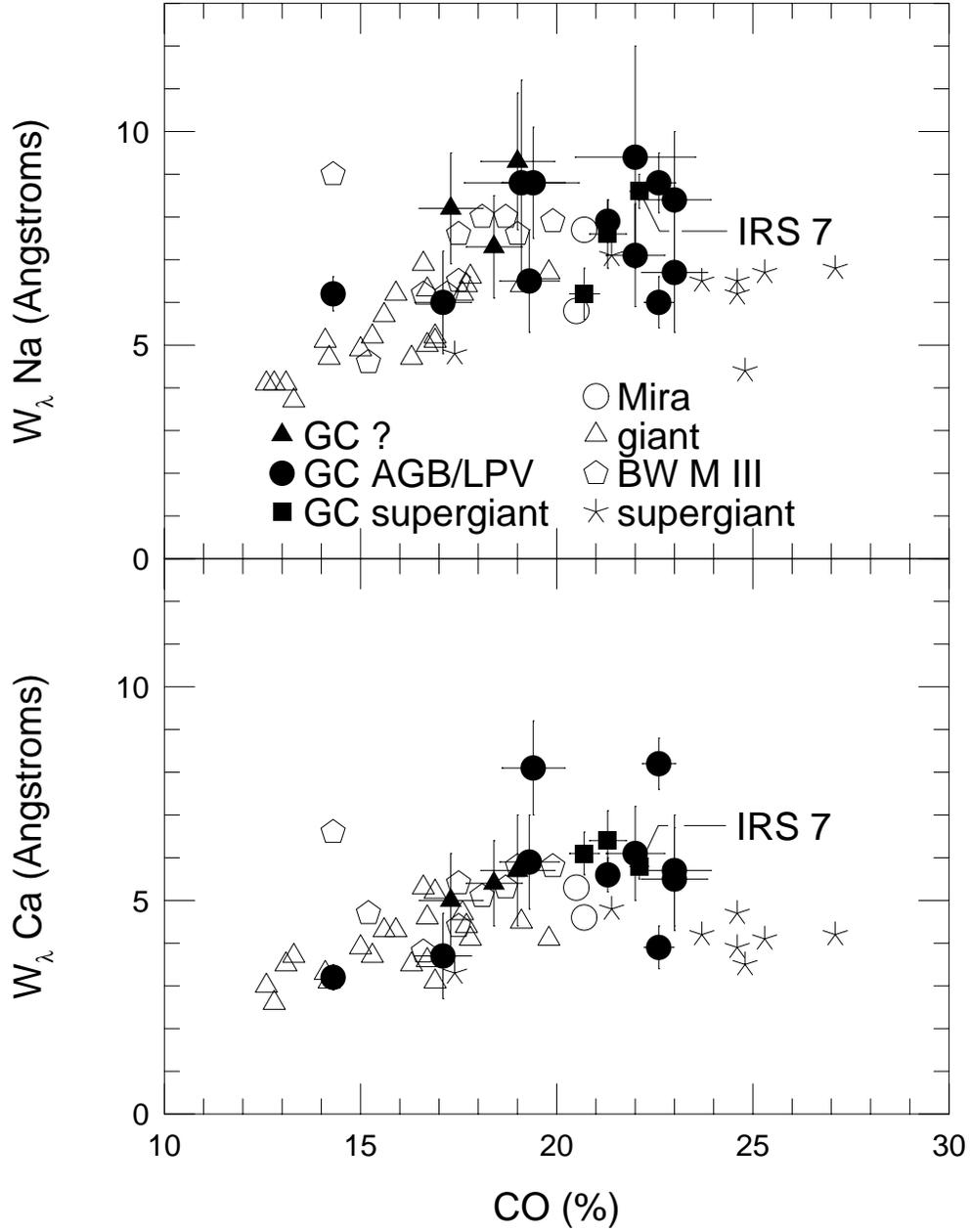
Fig. 4.— "Na" and "Ca" equivalent widths vs. CO strength. Symbols are the same as for Figures 2 and 3.

Fig. 5.— Color–magnitude diagram for the Galactic center (GC) cool stars and comparison stars. Individual data sets are described in Appendix 1. The GC stars are plotted in each panel along with known supergiants (*left panel*) and long period variables (LPVs) and M giants (*right panel*). IRS 7 is the most luminous GC star in the Figure. For clarity, not all the fainter stars in the Baade's window (BW) and LPV data sets are plotted. A sun-to-Galactic center distance of 8 kpc (Reid 1993) was adopted for the BW, Sgr I, and GC stars. The Large Magellanic Cloud (LMC) distance was taken as 46.8 kpc (Reid & Strugnell 1986). The error bars reflect photometric uncertainties in the derived de–reddened K magnitudes of Blum et al. (1996, Paper I). The effect of one magnitude of extinction at K is shown by the solid line according to the interstellar reddening curve of Mathis (1990). The red colors of the IRAS sources are due to circumstellar dust shells; see Appendix 1.
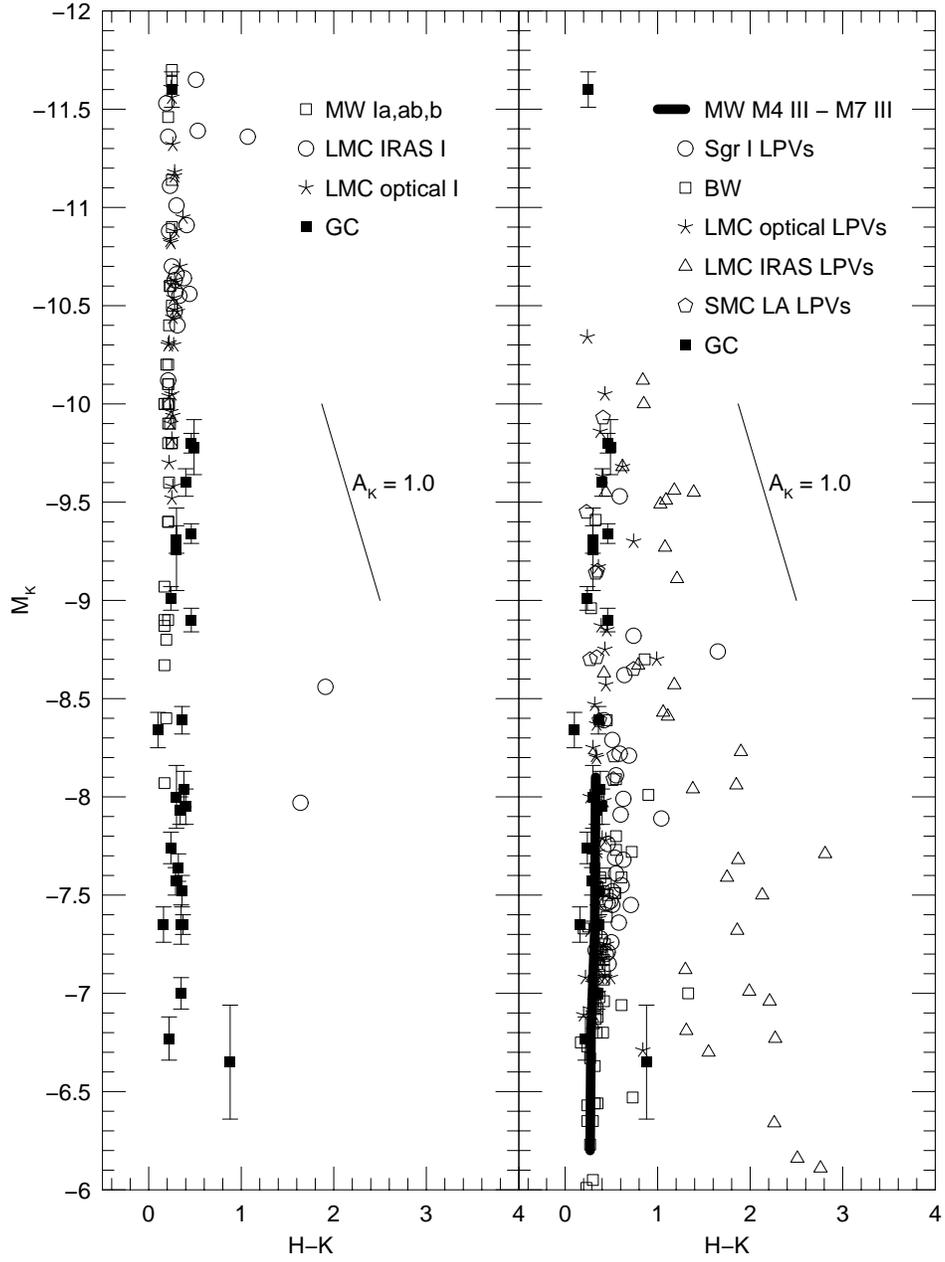
TABLE 2. Galactic Center Star Properties

Name	M_K[a]	$(H-K)_\circ$[b]	A_K[c]	M_{Kfaint}[d]	Type[e]	M_{bol}[f]	T_{eff}[g] (K)	M ($M_\odot$)[h]	Age (Myr)[h]
IRS 7	-11.60 ± 0.09	0.23 ± 0.11	3.48 ± 0.09	-10.12	SG	-9.0	3600	$20-25$	$7-9$
IRS 19	-9.80 ± 0.05	0.46 ± 0.06	3.50 ± 0.04	-8.30	SG	-7.2	3660	$12-15$	$12-18$
IRS 12N	-9.78 ± 0.14	0.49 ± 0.11	3.79 ± 0.14	-7.99	LPV	-6.5	2600	~ 5	~ 100
IRS 24[i]	-9.60 ± 0.07	0.40 ± 0.08	3.34 ± 0.06	-8.26	LPV	-6.4	2600	~ 5	~ 100
IRS 23	-9.34 ± 0.05	0.46 ± 0.06	3.44 ± 0.04	-7.90	LPV	-6.1	2600	~ 4	~ 200
IRS 9	-9.31 ± 0.07	0.30 ± 0.07	3.36 ± 0.06	-7.95	LPV	-6.1	2600	~ 4	~ 200
IRS 2	-9.26 ± 0.21	0.30 ± 0.18	5.31 ± 0.20	-5.95	?	$-6.8 - -6.1$	$3750 - 3210$	?	?
IRS 22	-9.01 ± 0.06	0.24 ± 0.07	2.52 ± 0.05	-8.49	SG	-6.4	3600	$9-12$	$18-29$
IRS 28	-8.90 ± 0.06	0.46 ± 0.06	3.74 ± 0.05	-7.16	LPV	-5.7	2800	~ 4	~ 200
IRS 14NE	-8.39 ± 0.07	0.36 ± 0.07	3.61 ± 0.05	-6.78	AGB	-5.2	3210	$2 - 4$	$190 - 1600$
IRS 11	-8.34 ± 0.09	0.10 ± 0.09	3.00 ± 0.06	-7.34	AGB	-5.1	< 3210	$2 - 4$	$190 - 1600$
OSU C3	-8.04 ± 0.09	0.38 ± 0.08	4.25 ± 0.09	-5.79	?	$-5.5 - -4.8$	$3600 - 3210$	?	?
IRS 1NE	-8.00 ± 0.16	0.30 ± 0.13	3.48 ± 0.14	-6.52	?	$-5.5 - -4.8$	$3750 - 3210$	?	?
F95 B	-7.95 ± 0.09	0.40 ± 0.09	3.32 ± 0.07	-6.63	$\cdots$	$\cdots$	$\cdots$	$\cdots$	$\cdots$
IRS 14SW	-7.93 ± 0.07	0.34 ± 0.07	3.56 ± 0.06	-6.37	$\cdots$	$\cdots$	$\cdots$	$\cdots$	$\cdots$
IRS 1SE	-7.74 ± 0.08	0.24 ± 0.07	3.47 ± 0.07	-6.27	?	$-5.2 - -4.5$	$3750 - 3210$	?	?
OSU C2	-7.64 ± 0.07	0.32 ± 0.07	3.22 ± 0.06	-6.42	AGB	-4.4	3210	$1 - 3$	$440 - 12000$
IRS 12S	-7.57 ± 0.07	0.29 ± 0.07	3.00 ± 0.06	-6.57	AGB	-4.3	3380	$1 - 3$	$440 - 12000$
OSU C4	-7.52 ± 0.08	0.36 ± 0.06	3.67 ± 0.07	-5.85	AGB	-4.3	< 3210	$1 - 3$	$440 - 12000$
OSU C1	-7.35 ± 0.10	0.35 ± 0.09	3.46 ± 0.10	-5.89	AGB	-4.1	3210	$1 - 3$	$440 - 12000$
IRS 10E	-7.35 ± 0.09	0.16 ± 0.09	3.19 ± 0.07	-6.16	$\cdots$	$\cdots$	$\cdots$	$\cdots$	$\cdots$
F95 J	-7.35 ± 0.05	0.37 ± 0.05	3.21 ± 0.04	-6.14	$\cdots$	$\cdots$	$\cdots$	$\cdots$	$\cdots$
IRS 20	-7.00 ± 0.08	0.35 ± 0.08	3.06 ± 0.06	-5.94	AGB	-3.8	3210	< 3	>440
IRS 33W	-6.77 ± 0.11	0.22 ± 0.11	3.12 ± 0.09	-5.65	$\cdots$	$\cdots$	$\cdots$	$\cdots$	$\cdots$
IRS 29S	-6.65 ± 0.29	0.88 ± 0.29	2.68 ± 0.08	-5.97	$\cdots$	$\cdots$	$\cdots$	$\cdots$	$\cdots$

[a]De–reddened K magnitude taken from Blum et al. (1996, Paper I). Uncertainty is a combination of photometric uncertainty in observed K and uncertainty in A_K (itself due to photometric uncertainty) added in quadrature. Distance to Galactic center taken as 8 kpc (Reid 1993).

[b]Taken from Blum et al. (1996, Paper I). $(H-K)_\circ$ follows from the observed $H-K$, the adopted extinction law (which gives the $E(H-K)$ in terms of A_K), and the derived A_K. A_K was first determined by assuming typical intrinsic $J-H$ and $H-K$ for M stars (IRS 1NE, 2, OSU C1, C3, and C4 had only $H-K$ measured). IRS 29S may have an excess at $H-K$ relative to $J-H$; see Blum et al. (1996, Paper I).

[c]Derived in Blum et al. (1996, Paper I) by assuming intrinsic colors for M stars; see note b. Uncertainty is photometric uncertainty only.

[d]Lower luminosity limit based on observed K and minimum A_K; see Appendix 1.

[e]Classification: SG, supergiant; LPV, shows strong H_2O and photometric variability; AGB, based on M_K, CO, and H_2O; ?, M_K and CO are consistent with either a SG or AGB classification. Spectral types are given in Table 1. Note that four stars have no spectrum analyzed in this paper. These four are identified as cool stars by Krabbe et al. (1995) and Figer (1995). Stars with "?" classifications are discussed further in § 4.

[f]Bolometric magnitude derived using $BC_K = 2.6$ and 3.2 for supergiants and LPV/AGB stars, respectively; see text and Appendix 1. Stars with "?" classifications have a range of bolometric magnitude corresponding to supergiant or AGB classification.

[g]Effective temperature, T_{eff}, from estimated spectral type (Table 1). See text for adopted T_{eff} vs. spectral type relations. Galactic center LPVs have T_{eff} estimated from M_{bol} and mass; see text. Stars with "?" classifications have a range of effective temperature corresponding to supergiant or AGB classification.

[h]Mass and age estimated from evolutionary models; see text. Values of mass and age for stars with "?" classifications are disscussed in the text.

[i]IRS 24 has been identified as an H_2O and OH maser source; see Appendix 2.